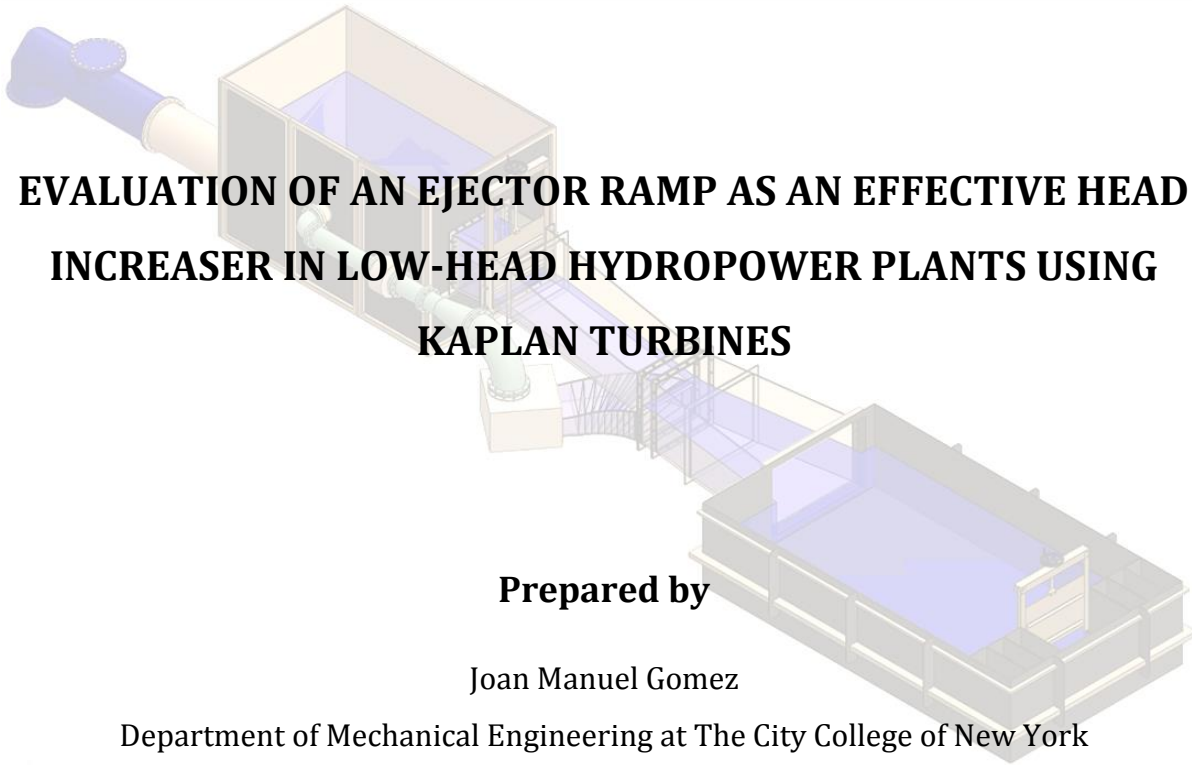# SUMMER RESEARCH REPORT

# EVALUATION OF AN EJECTOR RAMP AS AN EFFECTIVE HEAD INCREASER IN LOW-HEAD HYDROPOWER PLANTS USING KAPLAN TURBINES

## Prepared by

Joan Manuel Gomez

Department of Mechanical Engineering at The City College of New York

## Project Supervisors

Dr. Helmut Jaberg

Dr. Jürgen Schiffer

Institute for Hydraulic Fluid Machinery at Graz University of Technology

Summer 2014

# ACKNOWLEDGEMENT

First of all, I would like to thank Professor Dr. Helmut Jaberg for accepting my application to the Institute of Hydraulic Fluid Machinery and allowing me to be part of his team of experienced professors and highly motivated student. His valuable advices and explanations were very significant for my academic growth. Special thanks to Dr. Jürgen Schiffer, who not only guided me through this research period but also offered me his friendship and helped me with anything I needed during my stay in Graz. His clear explanations allowed me to easily understand the physical principles involved in this project and paved my way to carried out a successful research experience.

I also would like to thank Mrs. Katrin Landfahrer, who arranged everything for me in terms of the application process and paper work for the scholarship. Her constant assistance made it possible for my application to be review on time when I thought I was going to be out of the deadlines.

Thanks to the Marshall Plan Foundation for awarding me with the scholarship that made real this dreamed opportunity. I really appreciate their work since it not only represents and academic experience but also a cultural exchange that creates a remarkable experience in the students participating in this program.

Last but not least, thanks to the amazing people that I met in Graz and the faculty and staff of the Institute for Hydraulic Fluid Machinery at Graz University of Technology. All the help I received from them together with their advices on how to get the most out of my research period made this opportunity an unforgettable experience!

# ABSTRACT

Flood discharges exceeding a low-head hydropower plant capacity are usually not utilized and returned to the river as wasted discharge. In the present work, a method for the utilization of the otherwise wasted discharges exceeding the plant capacity is experimentally studied. In this case, part of the excess discharge is released through a spillway chute (ejector ramp) arranged over the draft tube. The physical principle is to mix the excess flow, or part thereof, with that leaving the draft tube and thus to transmit part of the kinetic energy inherent in the added high velocity jets to the slow discharge leaving the draft tube. The acceleration thus obtained is accompanied by a corresponding reduction in the pressure prevailing in the draft tube exit. The effect produced may be considered equivalent to lowering the tail water level, which increase the effective head for the turbine and therefore the total power output. Several experiments under different working conditions are performed and results are presented to validate the effectiveness of the ejector ramp. Numerical analysis is also carried out using Computational Fluid Dynamics (CFD) to compare results and to be used as an alternative to test the ejector ramp under different conditions.

# CONTENTS

# LIST OF FIGURES

# INTRODUCTION

The insolation of radiant energy supplied to the earth by the sun causes enormous quantities of terrestrial water to evaporate, and thus myriads of particles of water are lifted into the atmosphere as vapor. From hot climates, as well as from elsewhere, a substantial portion of vapor assembled in the atmosphere is then driven by incessant atmospheric currents towards lands.

In high altitudes, as soon as the ascending air masses chill to a certain point, the vapor condenses in the form of tiny drops of water and ice crystals. From the clouds thus formed the water precipitates to different parts of the earth as rain, snow or hail. At the last stage of what is known as the hydrologic cycle, the rain, thawing ice and snow constitute brooklets, rivulets, rivers and streams which carry the surface waters from different heights back to the seas and oceans.

Through ascension, that is, while evaporating from the seas into the atmosphere, the water masses gather potential energy, a portion of which is wasted in the process of precipitation from the clouds while the remainder is dissipated in the course of streaming in the river bed. [1]

Hydropower makes reference to the utilization of this energy available in moving water masses to convert it into a useful form of energy. In order to harness this energy dams are created with the objective of generate a head difference. This dammed water is then released, transforming its initial potential energy into kinetic energy. This moving flow passes through a turbine which transforms its kinetic energy into mechanical power that is later converted by a generator into electricity. According to the conditions of the river, different size of dams can be created and based on this generated head, hydropower plants are classified into different groups that go from high to low head. Hydropower plants also differ in the type of turbine utilize for the energy conversion. [2]

Finding different ways to satisfy our increasing energy demand, as well as achieving higher efficiency in our current energy conversion system is a daily challenge of engineers in a wide range of fields.

For this reason in the present work, the usage of an ejector ramp as an effective head increaser in low-head hydropower plants is analyzed. General explanation of this approach and the physics behind it is presented in the first chapter of the report together with a description of the water district available at the Institute for Hydraulic Fluid Machinery at Graz University of Technology. The approach is experimentally and numerically analyzed and the results obtained are presented in the second and third chapters. A comparison of the results and discussion is given in chapter fourth and the conclusions are presented are the end in the fifth chapter.

# 1. GENERAL DESCRIPTION.

## 1.1 Working principle of the ejector ramp.

The construction of hydropower plants implies an analysis of the flow rate and geographical conditions of the river where the power plant is to be built. However, during season of excessive rain there is a natural tendency of the rivers to increase their regular mass flow rate, exceeding the allowable flow rate that the turbine was design to handle. When this situation happens, the excess water is allowed to flow over the dam to be mixed with the downstream water and therefore is not utilized. As this water passes the weir it contributes to rapidly increase the tailwater level affecting the overall performance of the power plant. If the excess water keeps increasing, the head difference available at site decreases. If the available head falls out of the optimum head under which the turbine is designed to work, cavitation will appear and therefore the turbine needs to be shut down and the power generation will be interrupted.

With the objective of lessening the negative effect of the excess water, and on the contrary use it in the power plant's benefit, an ejector ramp could be implemented. An ejector ramp is a spillway chute arranged over the draft tube that allows the water discharges exceeding the plant capacity to flow down through it. The physical principle is to mix the excess flow, or part thereof, with that leaving the draft tube and thus to transmit part of the kinetic energy inherent in the added high velocity jets to the slow discharge leaving the draft tube. The acceleration thus obtained is accompanied by a corresponding reduction in the pressure prevailing in the draft tube exit. The effect produced may be considered equivalent to lowering the tail water level, which increase the effective head for the turbine and therefore the total power output. [1]

This increment in head difference may create a significant positive effect for the power plant, not only by increasing the power generation but also by allowing longer operation of the power plant during season of excessive rain. The analysis of this possible benefit is the objective of this project and will be discussed in detail in the following sections.

## 1.2 Description of the water district.

In order to perform experimental tests and analysis of the effect of the ejector ramp as a head increaser in low-head hydropower plants, a water district was already built in the Hydraulic Fluid Machinery experimental lab of the Graz University of Technology. The purpose of this water district

is to simulate the main characteristics of a low head hydropower plant. With total dimensions of 9 meters in length, 3 meters width and 1.8 meters height and no turbine included, this experimental structure facilitates the study of the behavior of the wake and head difference created when the water coming from the draft tube is mixed with the water that comes from the ejector ramp. Several conditions for the tail water level are tested in order to get a better understanding of the optimal operating conditions of this type of project.

As a first part of the project, a Computer-Aided Design (CAD) model was created with the objective of being used for future presentations and paper publications, as well as a basis for numerical analysis. In figure 1, the CAD model of the water district with its main components is shown.
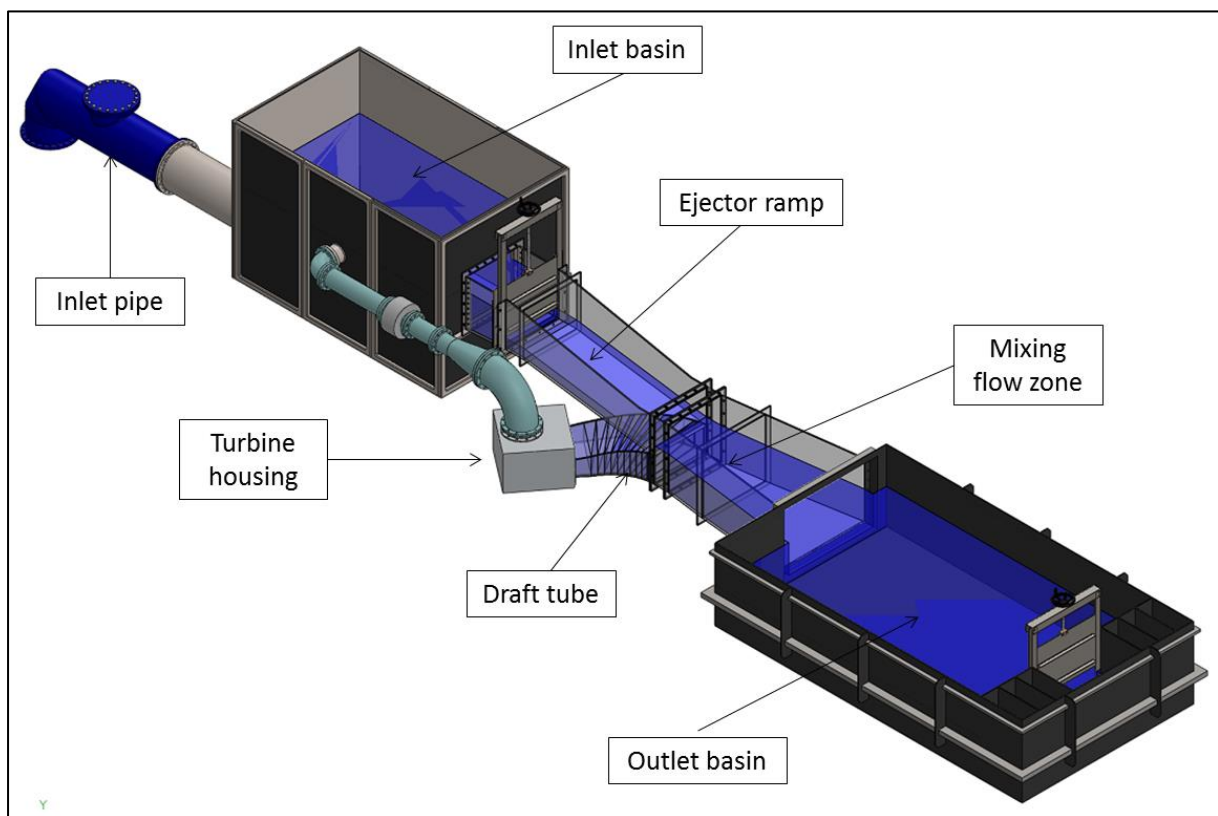


Figure 1. CAD model of the water district at the institute for Hydraulic Fluid Machinery – TU Graz

In this picture it is possible to explain how the water district works. The inlet water comes from the main pump and enters the system through the inlet pipe to fill up the tank to any desired level. The total flow in the system is controlled using a main panel that regulates the main pump's speed. Once the water is in the system, it flows through the turbine pipe getting to the turbine housing (where the turbine should be located if it was included in the system) and exits through the draft tube. Once

the water leaves the draft tube, it gets to the mixing zone where it meets the water that comes from the ejector ramp (located on top of the draft tube). The system also has an ejector gate that allows controlling the amount of water that goes from the inlet basin to the ramp. As a final step, the mixed water goes to the outlet tank and exits the system to start over the cycle.

In order to adjust the initial tail water to a desired level when the ejector gate is closed and the ramp is not working, a wooden weir with adjustable height was built in the outlet basin. This adjustable weir allows the development of experiments at different tail water levels. This in order to obtain a wide range of results that can simulate the working conditions of different low head hydropower plants in rivers with different tailwater characteristics.

In order to obtain valuable data from the water district, it is equipped with different types of sensor that are connected to a data acquisition system that can record several data points. Within the most relevant information taken from the system we have the following:

- $\Delta P_1$: Water pressure difference between the exit of the draft tube and the atmospheric pressure. (Figure2)
- $\Delta P_2$: Water pressure difference between the turbine pipe and the exit of the draft tube. (Figure 2)
- Upstream water level ($H_{high}$): Measured with respect to the tip of the ejector ramp nose and the water level in the inlet tank. (Figure 3)
- Tail water level ($H_{low}$): Measured with respect to the tip of the ejector ramp nose and the water level in the outlet tank. (Figure 3)
- Head difference: measured difference between upstream water level and tail water level.
- $Q_{Total}$: Total water flow coming in to the system through the inlet pipe.
- $Q_{Turbine}$: Total water flow in the turbine pipe.

Figure 2 shows the locations in the water district where $\Delta P_1$ and $\Delta P_1$ are measured. Figures 3 and 4 graphically show how the upstream and tail water levels are measured with respect to the tip of the ejector ramp nose, where the global coordinate system for the analysis is located.
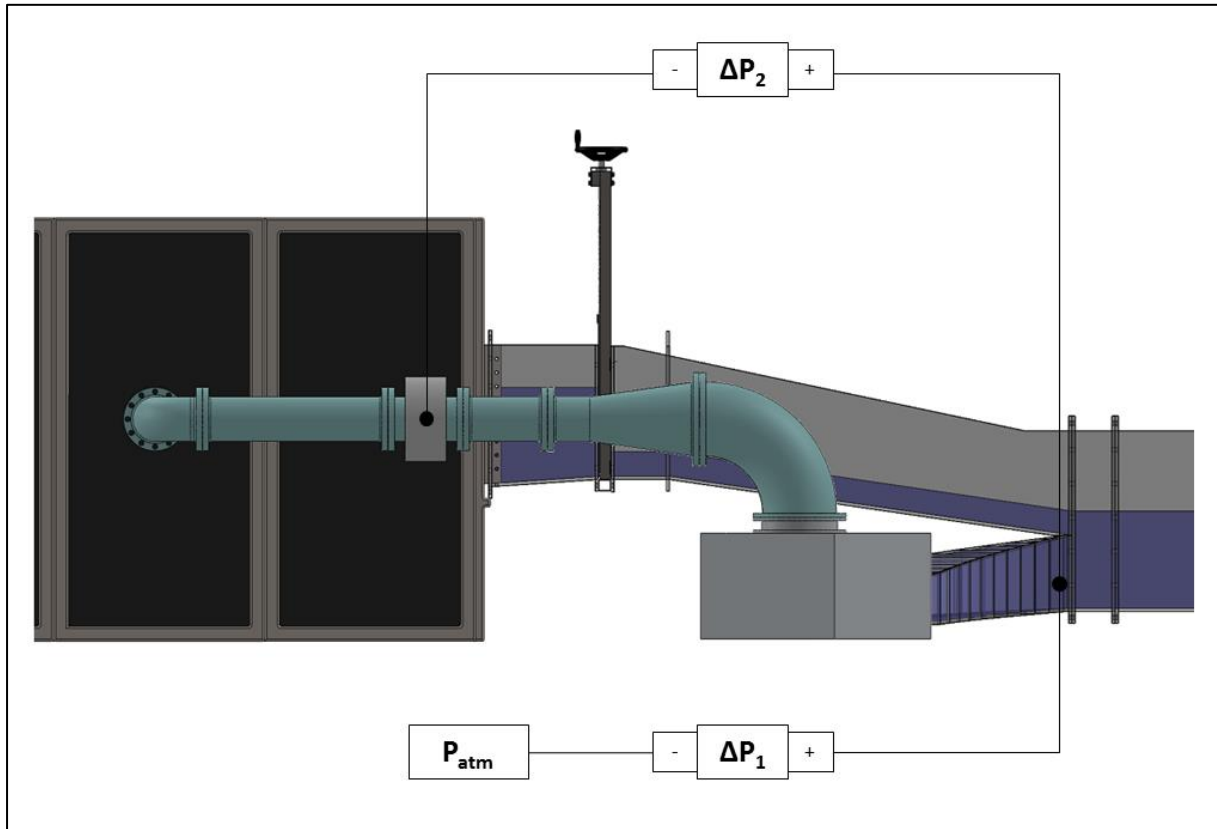
Figure 2. Position in the water district where $\Delta P_1$ and $\Delta P_2$ are measured.

In this figure it is shown a lateral view of the water district. In order to measure the pressure difference, this district is equipped with pressure transducers that sense pressure between two points and continuously sends the resulting signal to the data acquisition system. The signal that comes out of this pressure transducer is voltage and it is converted into pressure using a calibration matrix in the data acquisition board.

For the case of $\Delta P_1$, one measurement point takes water right at the wall of the exit of the draft tube at 180 millimeter below the tip nose. The other point is open to the atmosphere so it is full with air. Before starting any measurement, the pressure transducer needs to be flushed out for any remaining water in the system and to make sure that the measurements to be taken are correct.

For the case of $\Delta P_2$, one measurement point is taking a small amount of water from the turbine pipe and the other point is the same as the one used for $\Delta P_1$ which takes water at the exit of the draft tube.
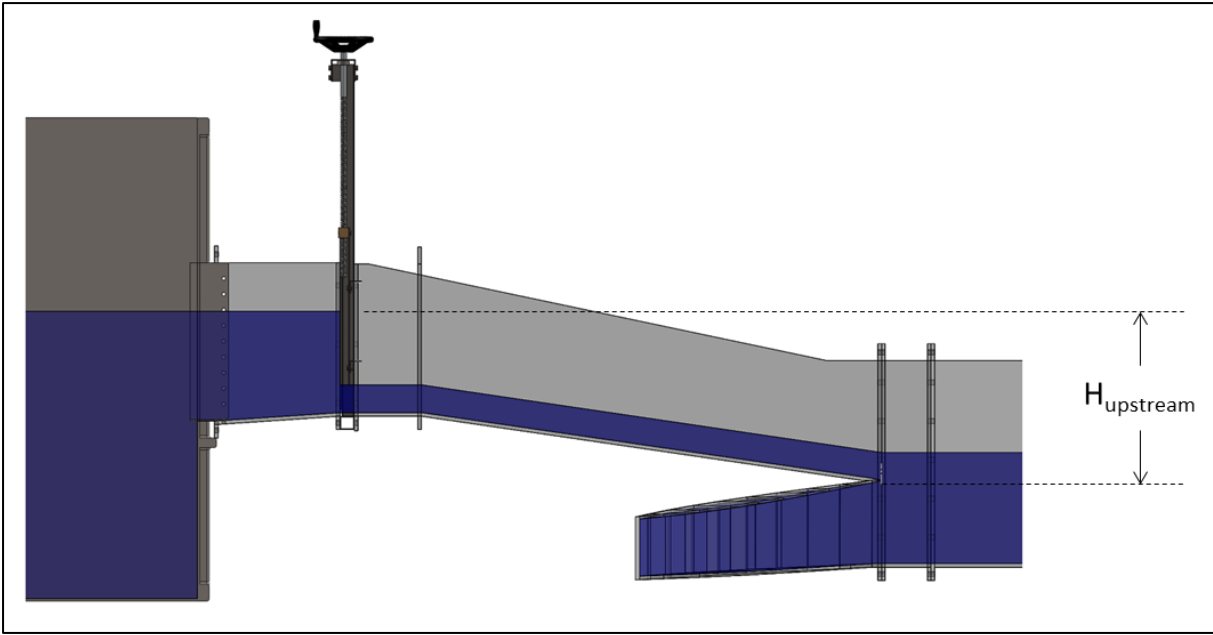
Figure 3. Measurement of the upstream water level.
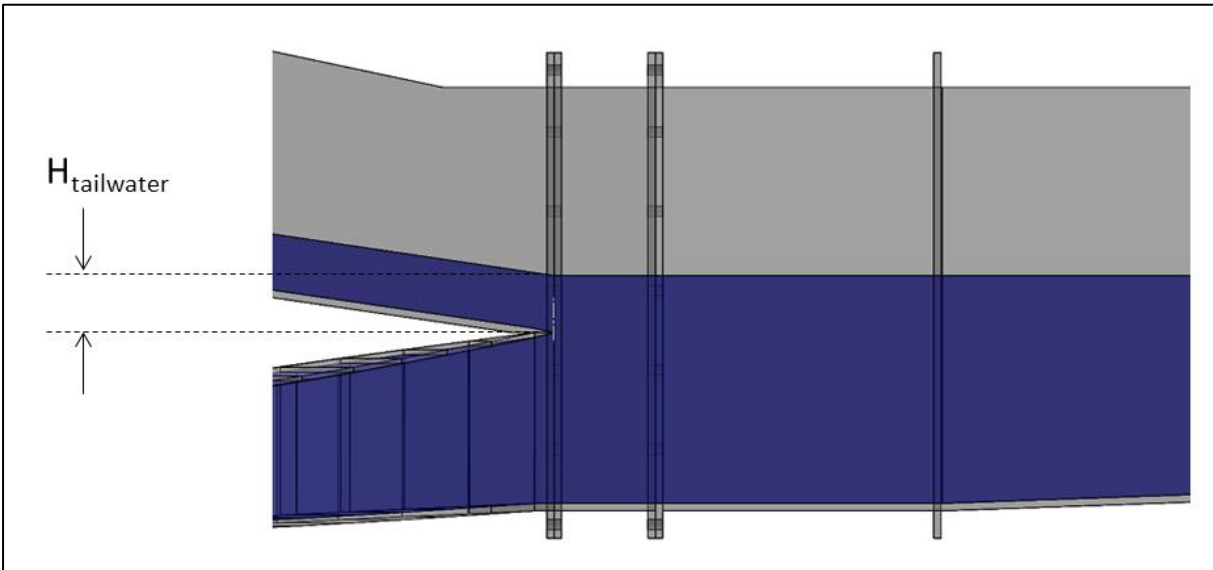


Figure 4. Measurement of the tailwater water level.

Another important parameter that needs to be measured is the location of the lowest point where the water from the ramp meets the water from the draft tube. These values need to be measured from the local coordinate system located at the tip nose of the ramp. The $x$ value which is measure along the horizontal axis represents how far from the nose the lowest point is located. The $y$ value which is measure along the vertical axis represents the actual head increment due to the ejector

effect. These values are visually obtained using a clear paper with calibrated lines to measure distances as shown in Figure 5.
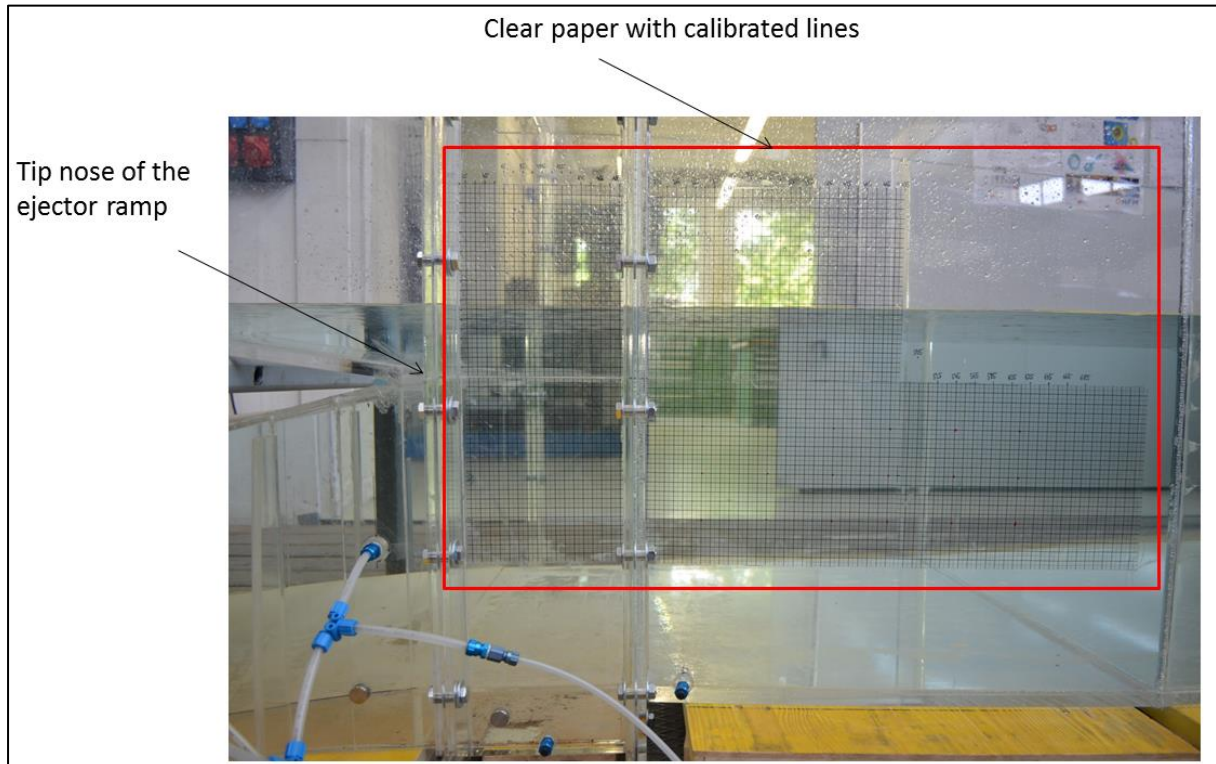


Figure 5. Visual measurement of the head increment due to the ejector effect.

Although this visual measurement introduces a source of uncertainty, it is the only way to identify the location of this lowest point. The values taken are every different total flow rate will differ significantly from each other and therefore high precision is not strictly required. For this reason the measurements taken with this method are considered valid enough for the purpose of this study.

## 2. EXPERIMENTAL ANALYSIS

### 2.1 EJECTOR GATE CLOSED.

The first set of experiments carried out consisted in a characterization of the flow when the ejector gate is closed and hence there is no water flowing through the ejector ramp. The experiments are performed by increasing the total flow rate in the system to measure important flow information.

The main objective of this first set of experiments is to obtain a correlation equation that can help to compare the results from experiments when the ejector gate is closed and opened. The idea is to clearly appreciate the overall effect of the ejector ramp in the hydropower plant.

As a first correlation equation, it was decided to use the head difference ($H_{high} - H_{low}$) as an independent variable. The reason for this is that the head difference is a characteristic that is common to all the experiments and therefore it is present even when the experiment is performed with the ejector ramp active. Figure 7 shows the turbine flow rate in terms of the head difference when water is not flowing down the ejector ramp.
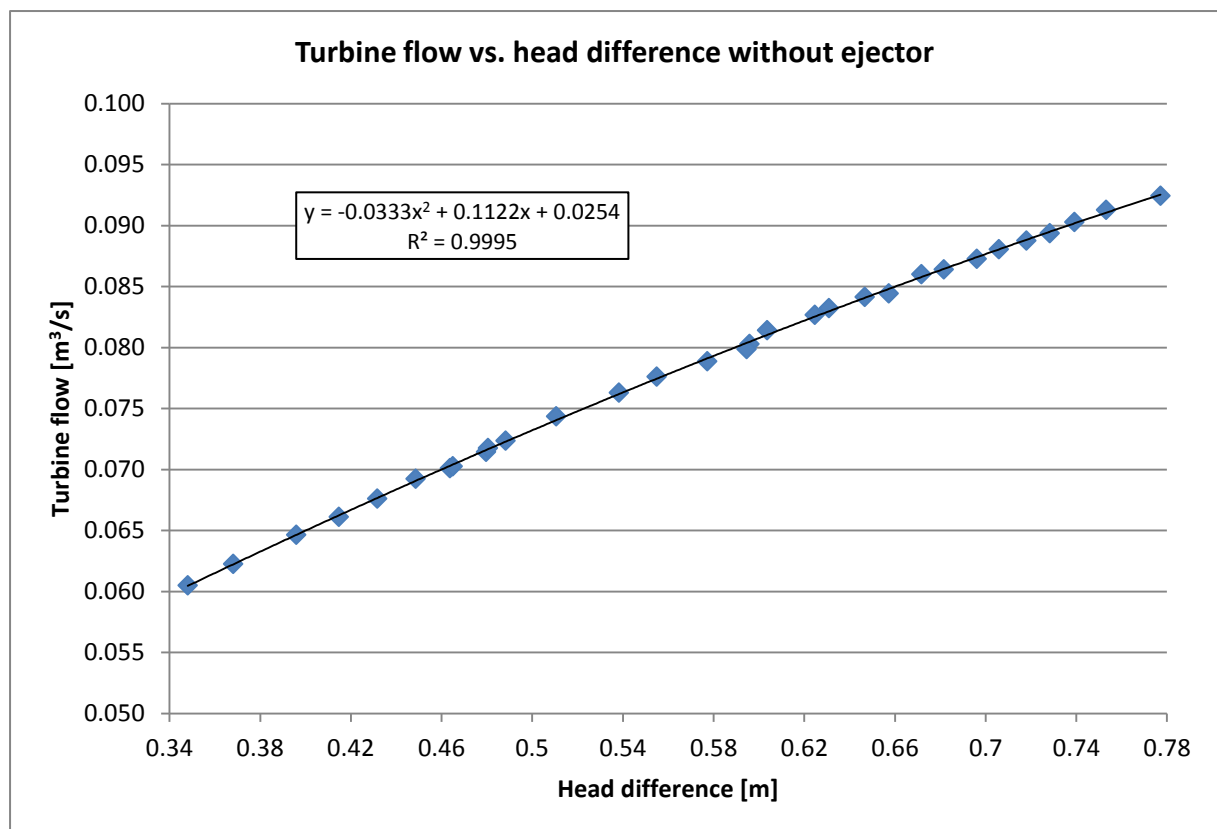


Figure 6. Experimental correlation between turbine flow and head difference when the ejector is not implemented.

In this figure, we can also see the quadratic equation for the trend line together with the R-squared value, which shows that the trend line fits with good agreement the data points. This equation will be later used for comparison with the results when the ejector gate is opened.

An important parameter that is also considered is the water drop height, which is calculated using Bernoulli's equation. The water drop height will be considered as the effective head and will be used to calculate the theoretical hydraulic power. Figure 8 shows the schematic used for the calculation, where a local coordinate system is conveniently located in the point O at the exit of the draft tube, which is where the pressure is being measure by the data acquisition system in relation with the atmosphere pressure ($\Delta P_1$).
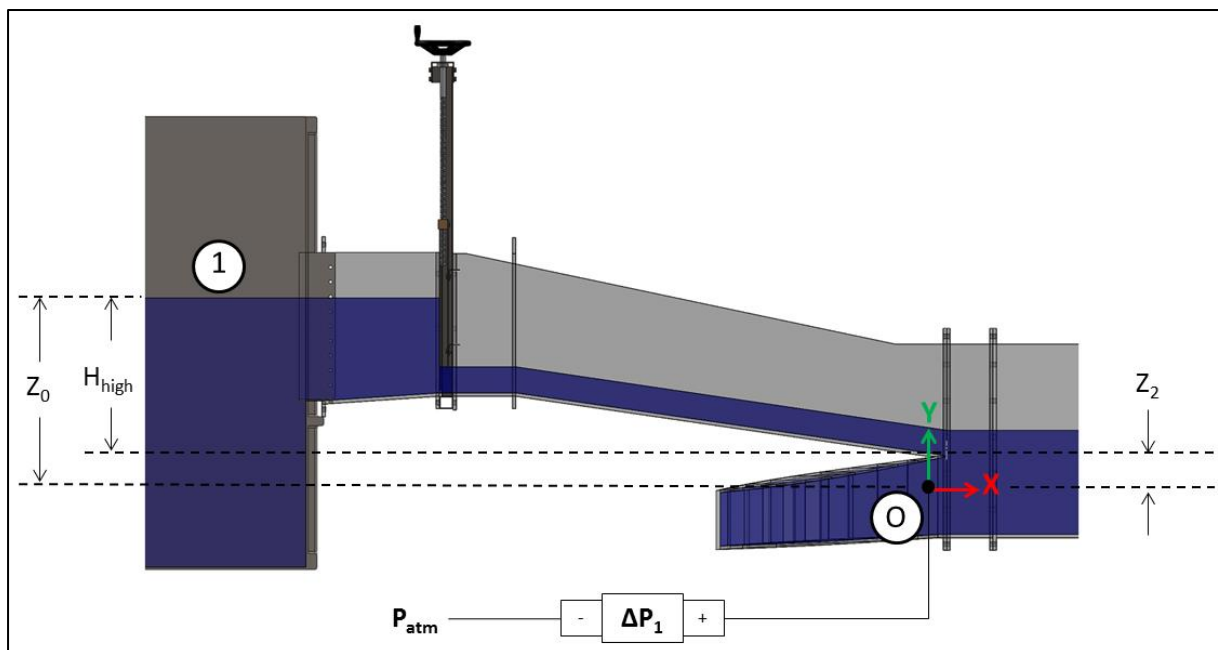


Figure 7. Schematics used to calculate the drop height using Bernoulli's equation.

The water drop height is calculated between the upstream water level (Point 1) and the location of the local coordinate system (Point O) shown in figure 8. Although the defined local coordinate system is used as a reference for the calculation, some of the distances are taken with respect of the tip nose (global coordinate system) because their values with respect to this point are already known.

In figure 8, $H_{high}$ is the vertical distance from the tip nose to the upstream water (Point 1), $Z_0$ is the vertical distance between Point 0 and Point 1, and $Z_2$ is the vertical distance from the point O to the tip nose of the ejector. The procedure used for the calculation is the following

$$H = h_1 - h_2$$

Where $H$ is the water drop height, $h_1$ is the equivalent head of the point 1 and $h_2$ is the equivalent head of Point O. Bernoulli's equation for each of these points writes

$$h_1 = \frac{P_{atm}}{\rho g} + \frac{V_1^2}{2g} + Z_0$$

$$h_2 = \frac{P_o}{\rho g} + \frac{V_o^2}{2g} + 0$$

Therefore we have

$$H = \frac{P_{atm}}{\rho g} + \frac{V_1^2}{2g} + Z_0 - \frac{P_o}{\rho g} - \frac{V_o^2}{2g} - 0$$

Rearranging

$$H = \frac{P_{atm} - P_o}{\rho g} + \frac{V_1^2 - V_o^2}{2g} + Z_0 - 0$$

Because $\Delta P_1$ is measured by the system, it will be included to simplify the calculation. As it was previously explained, $\Delta P_1$ is the pressure difference between the static pressure of the water at the exit of the draft tube and the atmospheric pressure. Mathematically we can write this as follows

$$\Delta P_1 = P_o - P_{atm}$$

Replacing these equations we have

$$H = -\frac{\Delta P_1}{\rho g} + \frac{V_1^2 - V_o^2}{2g} + Z_0$$

Now, as the point 1 is located at the surface in the inlet tank, it is assumed that the velocity at that point is very small and can be neglected ($V_1 = 0$). Rearranging we have

$$H = -\frac{\Delta P_1}{\rho g} - \frac{V_o^2}{2g} + Z_0$$

We also have

$$Z_0 = H_{high} + Z_2$$

and

$$V_o = \frac{Q_{turbine}}{A}$$

Where $Q_{turbine}$ is measured for the acquisition system and $A$ is the cross sectional area of the draft tube which can be computed from its dimensions that are already known.

Replacing we finally have

$$H = -\frac{\Delta P_1}{\rho g} - \frac{(Q_{turbine})^2}{2g(A)^2} + H_{high} + Z_2$$

In this equation $\Delta P_1$, $Q_{turbine}$ and $H_{high}$ are variables that are measured by the data acquisition system, $\rho$ is the density of the water and $g$ is the gravity which are constants that are already known together with $A$. At this point, all the terms are ready for the calculation of the water drop height.

Now that the water drop height can be calculated, it will be also used to obtain a second correlation equation for comparisons with the case when the ejector is being implemented. Figure 9 shows the water drop height in terms of the head difference when water is not flowing down the ejector ramp. This figure also shows the quadratic equation for the trend line together with the R-squared value. In this case we also have that the trend line fits with good agreement the data points and can be used for comparison purposes.
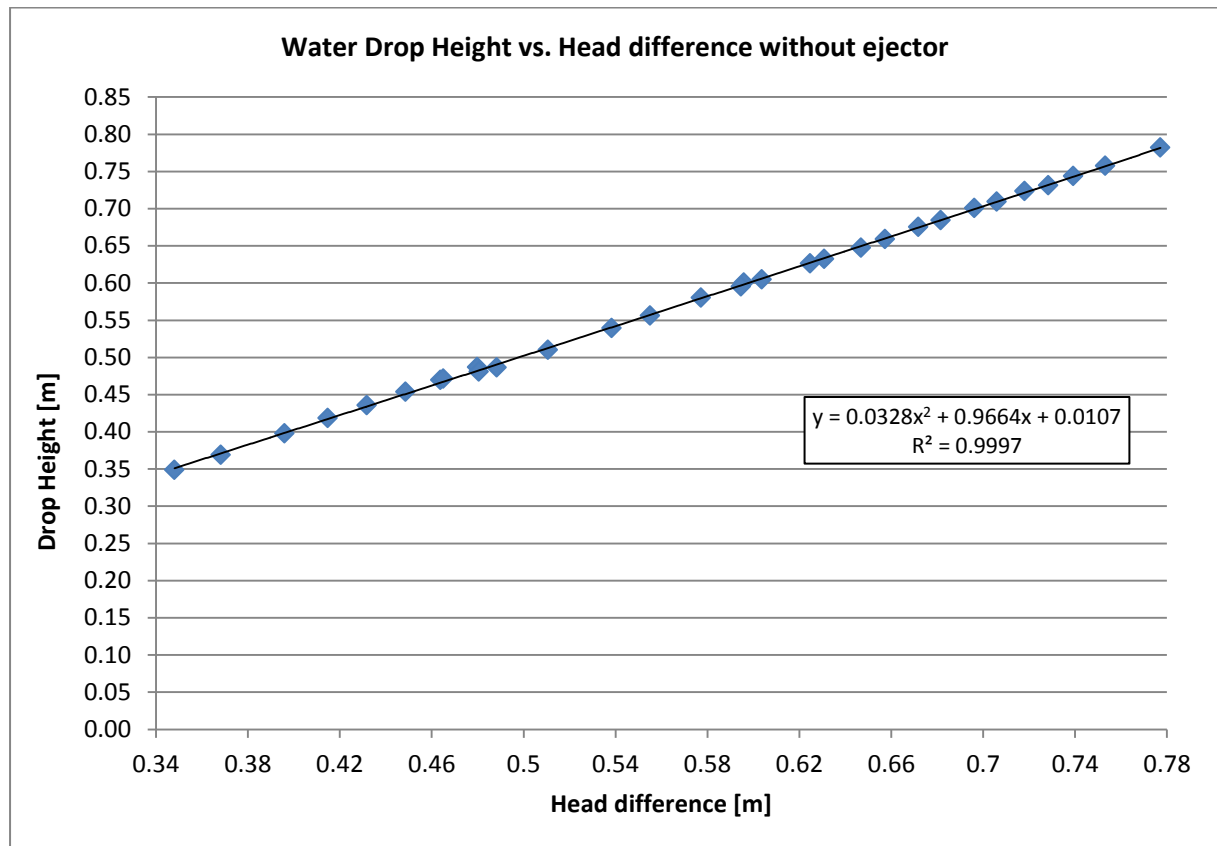


Figure 8. Experimental correlation between water drop height and head difference when the ejector ramp is not implemented.

11

Once these equations from the results of the experiments with the ejector ramp closed are obtained, we can proceed to perform the experiments with water flowing down the ramp and compare the results.

## 2.2    EJECTOR GATE OPENED.

Experiments with the ejector gate opened are performed in the same conditions as for the case with the gate closed. The total flow rate going in to the system is increased. The only difference is that in this case as the total flow increases the ejector gate is opened to allow more water in the ramp and at the same time keep the upstream water level constant at 700 millimeters.

As it was mentioned before, the tailwater behaves differently for each hydropower plant depending on the river characteristics. For this reason, different experiments are performed at different initial tailwater levels. This allows obtaining results than can be adjusted to a wider range of low-head hydropower plants and a better understanding of the effectiveness of the ejector ramp at different tailwater characteristics.

Five different initial tailwater levels were analyzed. Since the water level in the draft tube cannot be excessively low to avoid cavitation to occur in the turbine, only one experiment was carried out with tailwater level below the tip nose of the ramp. The other four experiments correspond to tailwater levels at and above the tip nose.

### 2.2.1    Tail water level at the tip nose (0 millimeters elevation)

The first experiment was performed keeping the initial tail water level at the tip nose. Figures 9 and 10 show the main results obtained.

Figure 9 shows the trend of the results for the upstream water level, tailwater level, and head difference (difference between the upstream water level and the tailwater level) obtained.

Figure 10 shows the water drop height computed using the equation that was obtained from Bernoulli's equation and the water drop height without ejector which is calculated using the second correlation equation (Figure 8). It also shows the pressure $\Delta P_1$ which is seen to decrease with increasing total flow while the water drop height with ejector increases. Since the head difference decreases with increasing total flow as seen in Figure 9, it is expected that the water drop height without ejector shows the same behavior.
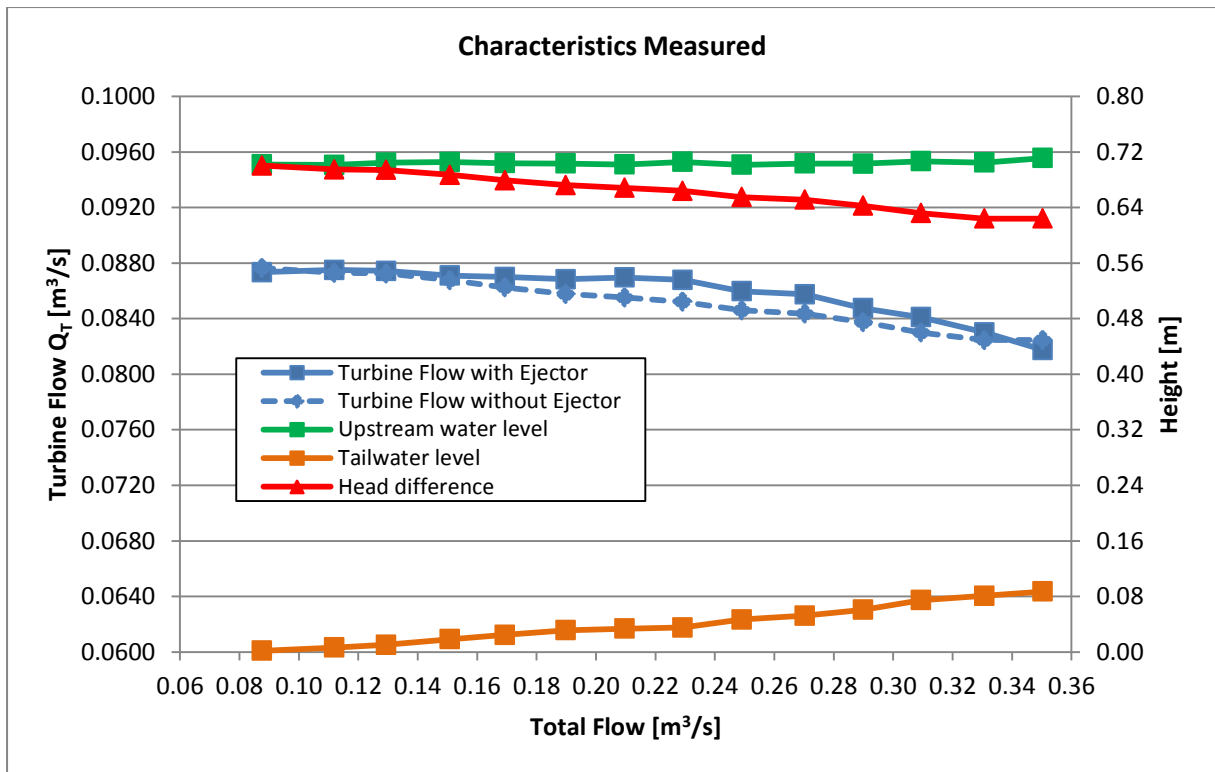
Figure 9. Characteristics measured with initial tailwater level at the tip nose.
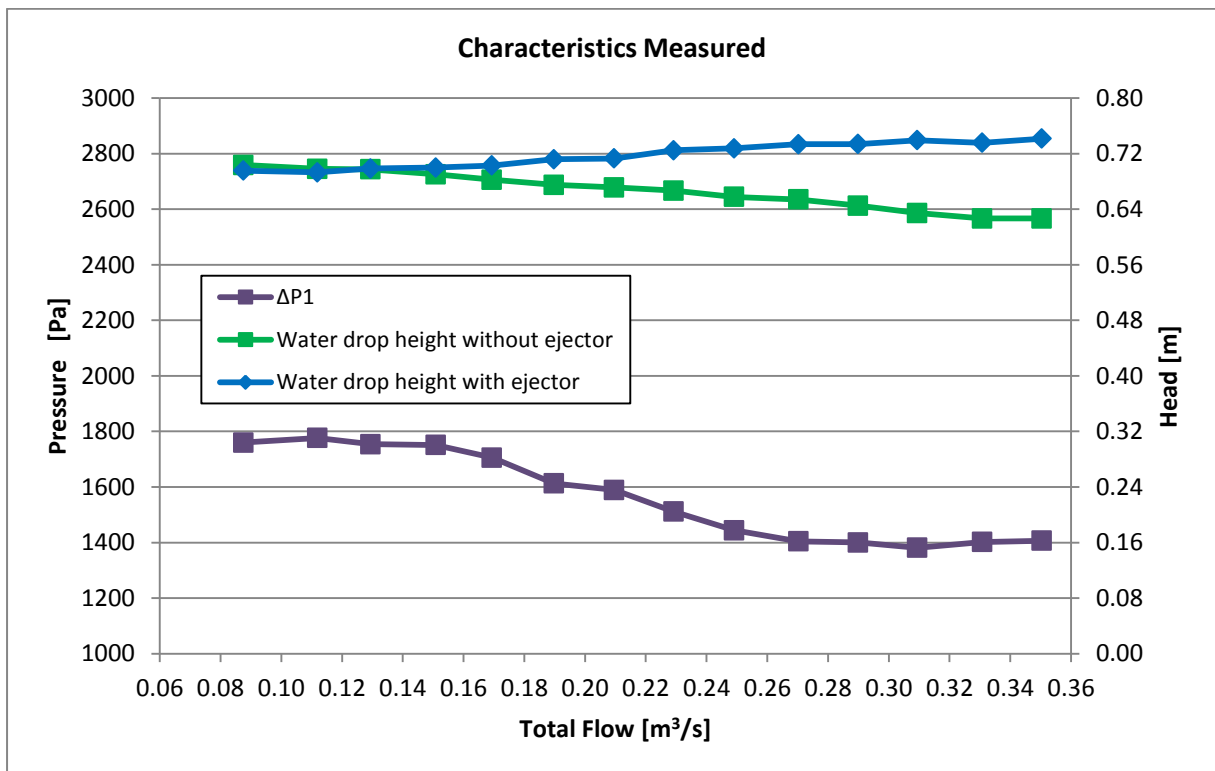


Figure 10. Characteristics measured with initial tail water level at the tip nose.

In figure 9 it is possible to see that as the total flow increases the tail water level rapidly increases from 0 to approximately 0.1 meters. Since the upstream water level is kept constant, the head difference decreases as the tailwater rises with increasing total flow. This figure also shows the turbine flow measured with the data acquisition system and the turbine flow without ejector, which is calculated using the first correlation equation (Figure 7) obtained previously for the case when the ejector gate is closed.

We can see in this figure that the turbine flow with ejector is higher than the calculated turbine flow without ejector at almost every different total flow rate. This is due to the decrease in pressure at the outlet of the draft tube ($\Delta P_1$) when the exiting flow is mixed with the water coming from the ejector ramp. This decrease in pressure makes more water to flow through the turbine pipe and thus the increment in turbine flow when the ejector ramp is active

As a final step, the hydraulic power is calculated using the following expression

$$P_{Hyd} = \rho \cdot g \cdot Q_{Turbine} \cdot H_{wdh}$$

Where $\rho$ is the density of water, $g$ is the acceleration of gravity, $Q_{Turbine}$ is the turbine flow rate, and $H_{wdh}$ is the water drop height. Figure 11 shows the hydraulic power as a function of the total flow rate when the ejector gate is opened (ramp active) and when the ejector gate is closed.
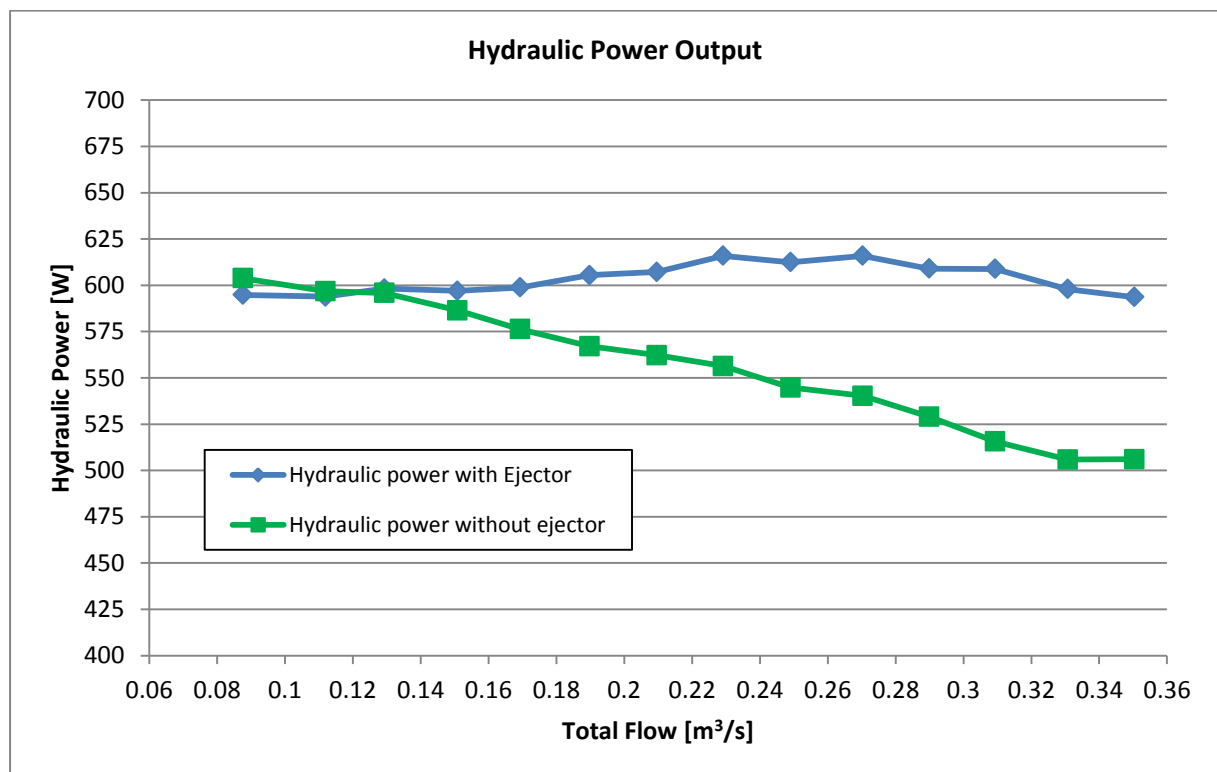


Figure 11. Hydraulic power output with initial tail water right at the tip nose.

In this figure it can be seen that the power without ejector decreases when the total flow increases. In contrast, the hydraulic power when the ejector is implemented shows an increment from 0.23 $m^3$/s to 0.27 $m^3$/s. Beyond this value of total flow rate the power decreases slightly. However, the hydraulic power with ejector is higher than the calculated power without ejector. According to these results, the ejector ramp has a positive effect as an effective head increaser and at the same time allows the power plant to generate more power.

### 2.2.2 Tail water level 30 millimeters below the tip nose of the ejector ramp

In this case the experiment is performed in the same manner that was used for the previous case. The only difference is the initial tail water level which is lower. Figure 12 shows the results for the main characteristics measured. In this case we can see a different tailwater behavior. Although it tends to increase as the total flow is higher, there is a point at 0.23 $m^3$/s where it stabilizes and stays constant at the same level. It can be noted that the amount of increment in the tailwater level is lower than in the previous case. The tailwater level increases from -0.03 meters to around 0.01 meters at the maximum total flow tested. We can also see that in this case the turbine flow with ejector is slightly higher than the case without ejector. However, at 0.27 $m^3$/s the turbine flow with ejector decreases and goes below the turbine flow rate without ejector.



Figure 12. Characteristics measured with initial tail water level 30 mm below the tip nose.

Figure 13 shows the water drop height with ejector and the calculated water drop height without ejector and figure 14 shows the hydraulic power calculated for this case.



Figure 13. Characteristics measured with initial tail water level 30 mm below the tip nose.



Figure 14. Hydraulic power output with initial tail water level 30 mm below the tip nose.

According to figure 9, we see that in this case the values for this characteristic are higher when the ejector ramp in implemented. The pressure difference $\Delta P_1$ decreases as it was seen in the previous case. However, at 0.27 m³/s it starts increasing. This increment in pressure at the outlet of the draft tube is responsible for the decrease in turbine flow rate with ejector that was seen in Figure 12.

As for the hydraulic power we see that in this case we also have that the hydraulic power with ejector is higher than the one calculated for the case without ejector.

This result once more shows a positive effect of the ejector ramp as an increaser of effective head and hydraulic power.

### 2.2.3 Tail water level 40 millimeters above the tip nose of the ejector ramp

This experiment is performed following the same procedure. Figure 15 shows the main characteristics measured. In this figure it is seen that the tailwater level increases from 0.04 meters to around 0.1 meters at the maximum total flow tested, which means a steeper slope than in the previous case. We can also see that in this case the turbine flow with ejector is almost the same than in the case without ejector.
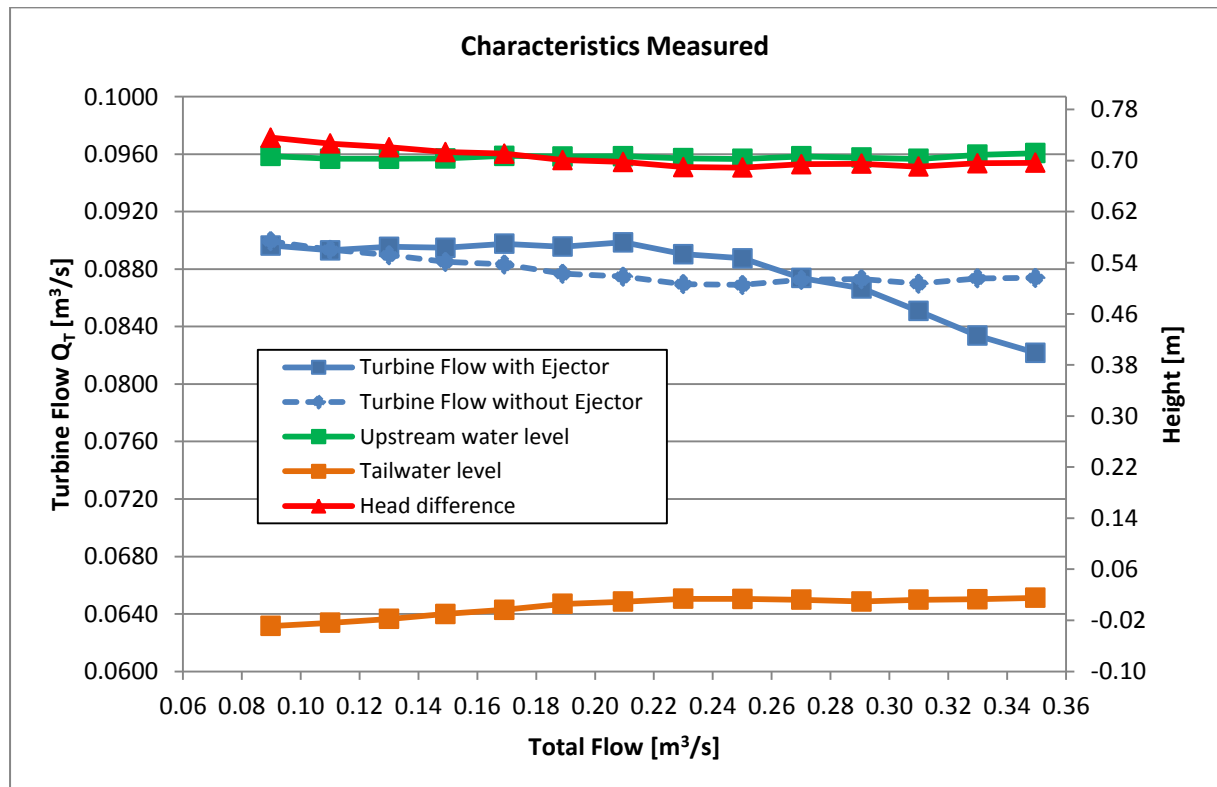


Figure 15. Characteristics measured with initial tail water level 40 mm above the tip nose.

In Figure 16 it is shown the water drop height with ejector and the calculated water drop height without ejector. Figure 17 shows the hydraulic power obtained in this case.
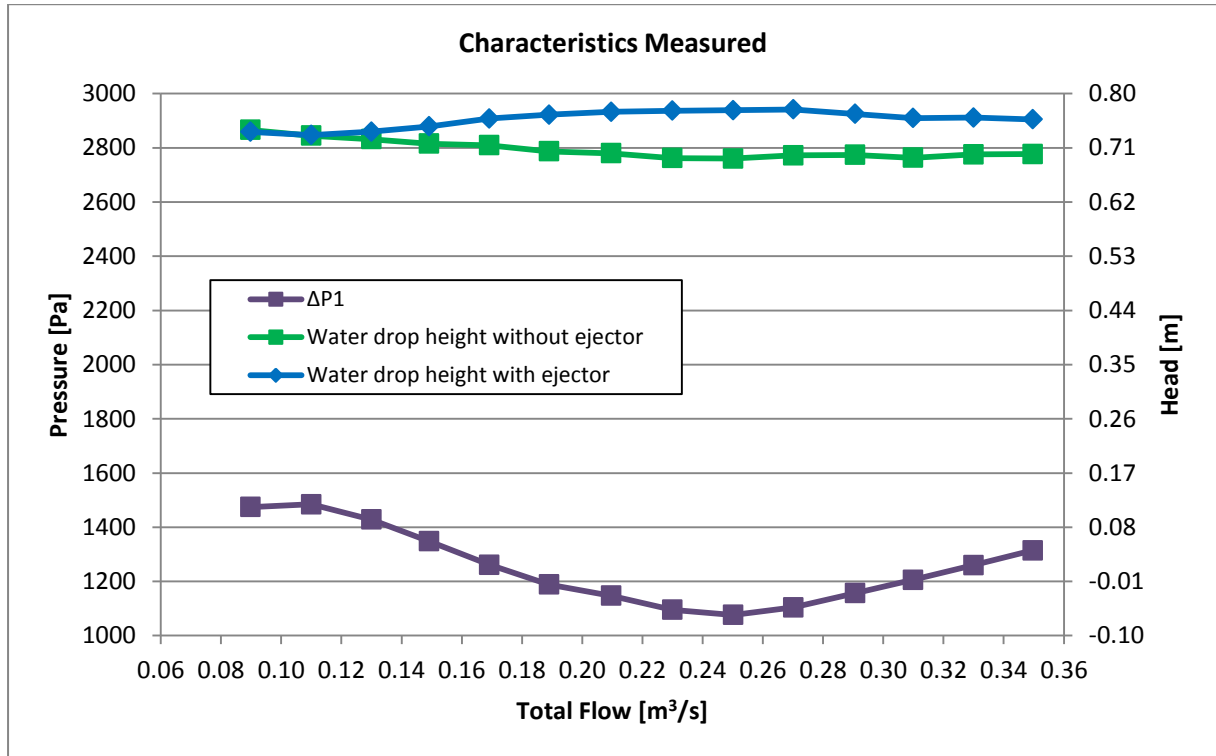


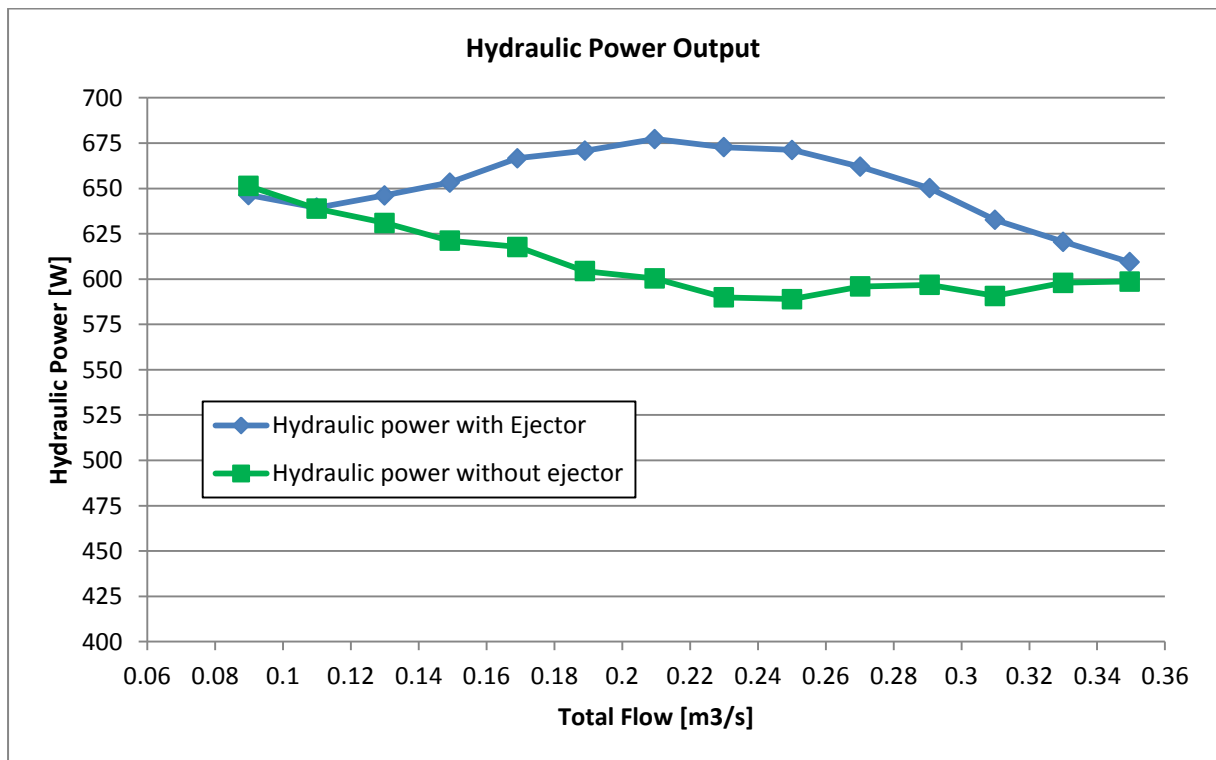Figure 16. Characteristics measured with initial tail water level 40 mm above the tip nose.



Figure 17. Hydraulic power output with initial tail water level 40 mm above the tip nose.

As it is seen in figure 16, in this case the water drop height is higher when the ejector ramp in implemented and the pressure difference ΔP1 decreases as it was seen in the previous cases.

The hydraulic power is calculated using the same procedure as before. It is possible to see in figure 17 that the hydraulic power with ejector is higher than the one calculated for the case without ejector, showing again positive results on the effect of the ejector ramp as a head and power increaser.

### 2.2.4 Tail water level 60 millimeters above the tip nose of the ejector ramp.

Once again the experiment is carried out using the same approach as before. Figure 18 shows the main characteristics measured. This figure shows that the tailwater level increases from 0.06 meters to around 0.13 meters at the maximum total flow. In this case we have that the turbine flow with ejector is lower than the turbine flow rate without ejector.
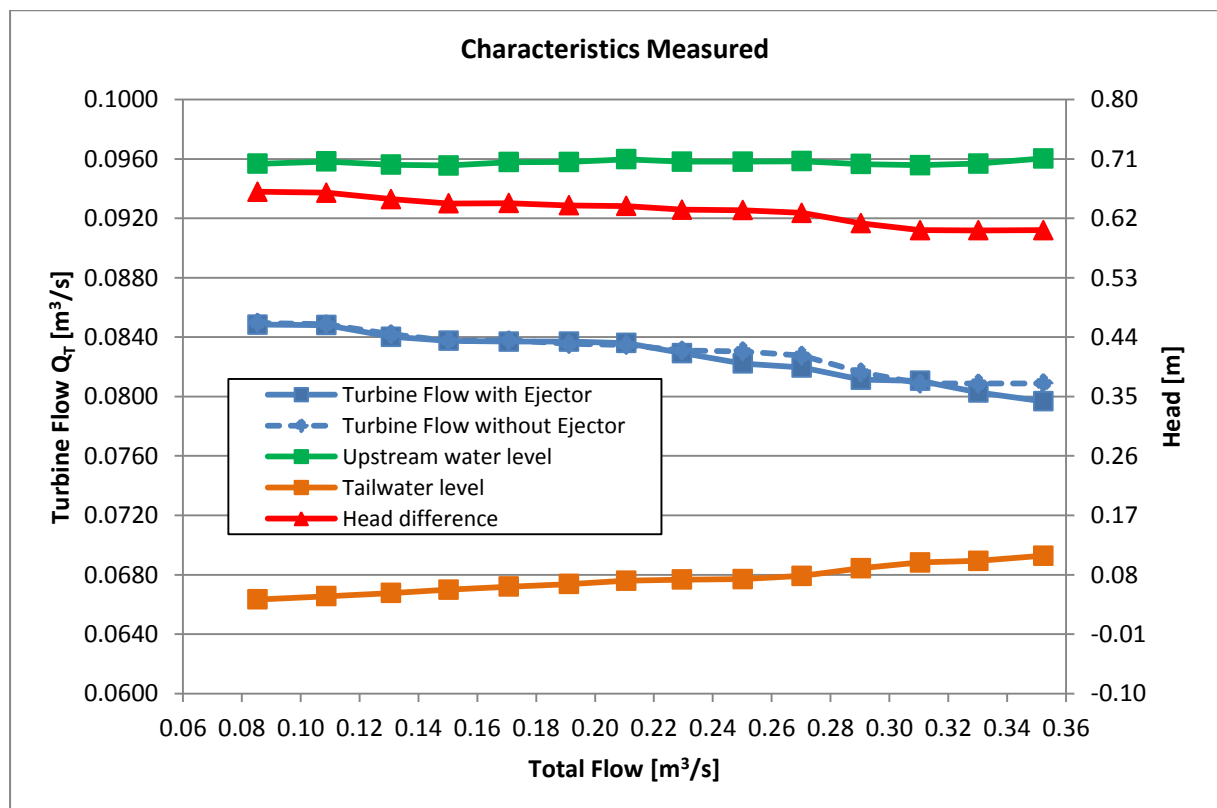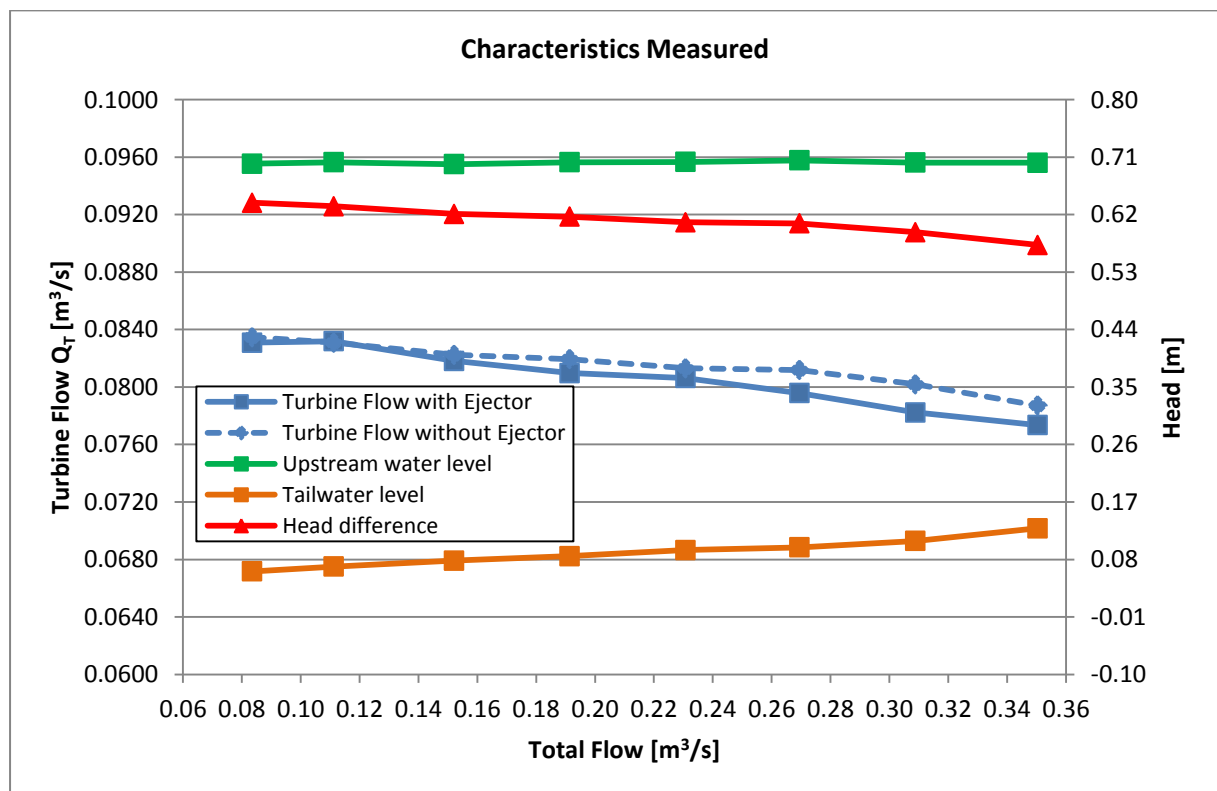


Figure 18. Characteristics measured with initial tail water level 60 mm above the tip nose.

Figure 19 shows the water drop height with ejector and the calculated water drop height without ejector. As in the previous cases, the water drop height is higher when the ejector ramp in implemented and the pressure difference $\Delta P_1$ decreases with increasing total flow rate. Figure 20 shows the hydraulic power computed for this case.
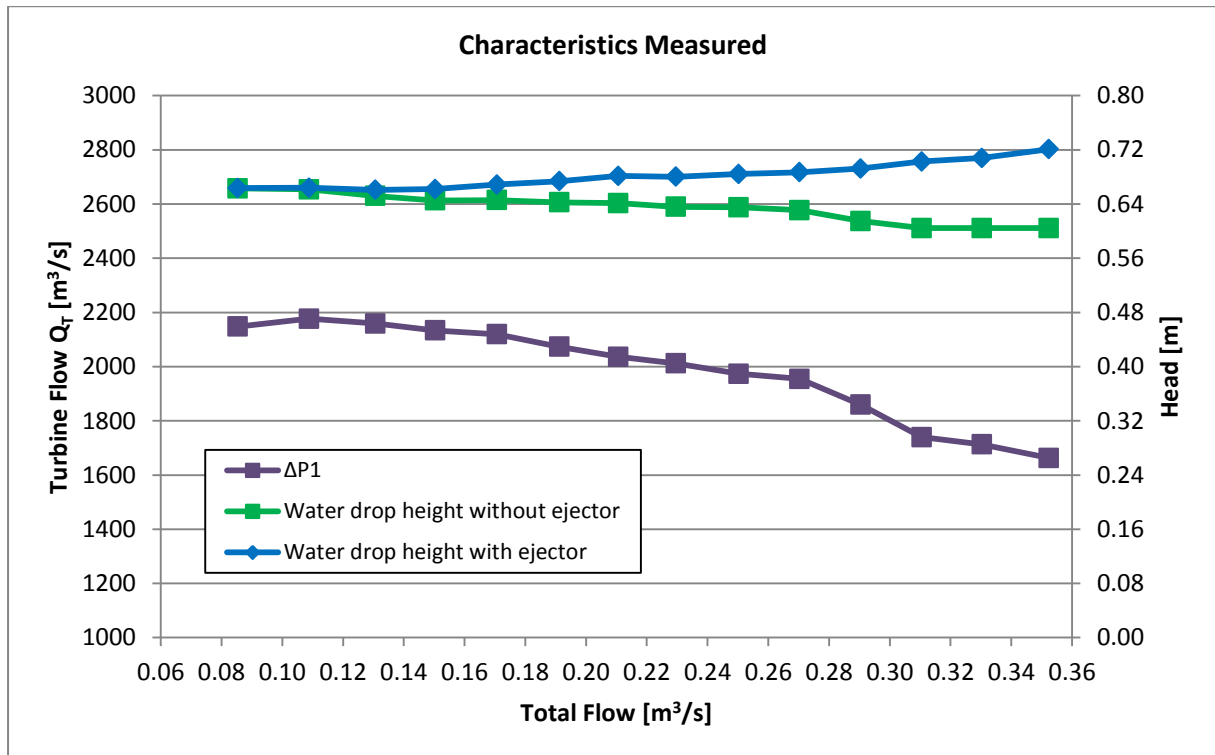
Figure 19. Characteristics measured with initial tail water level 60 mm above the tip nose.
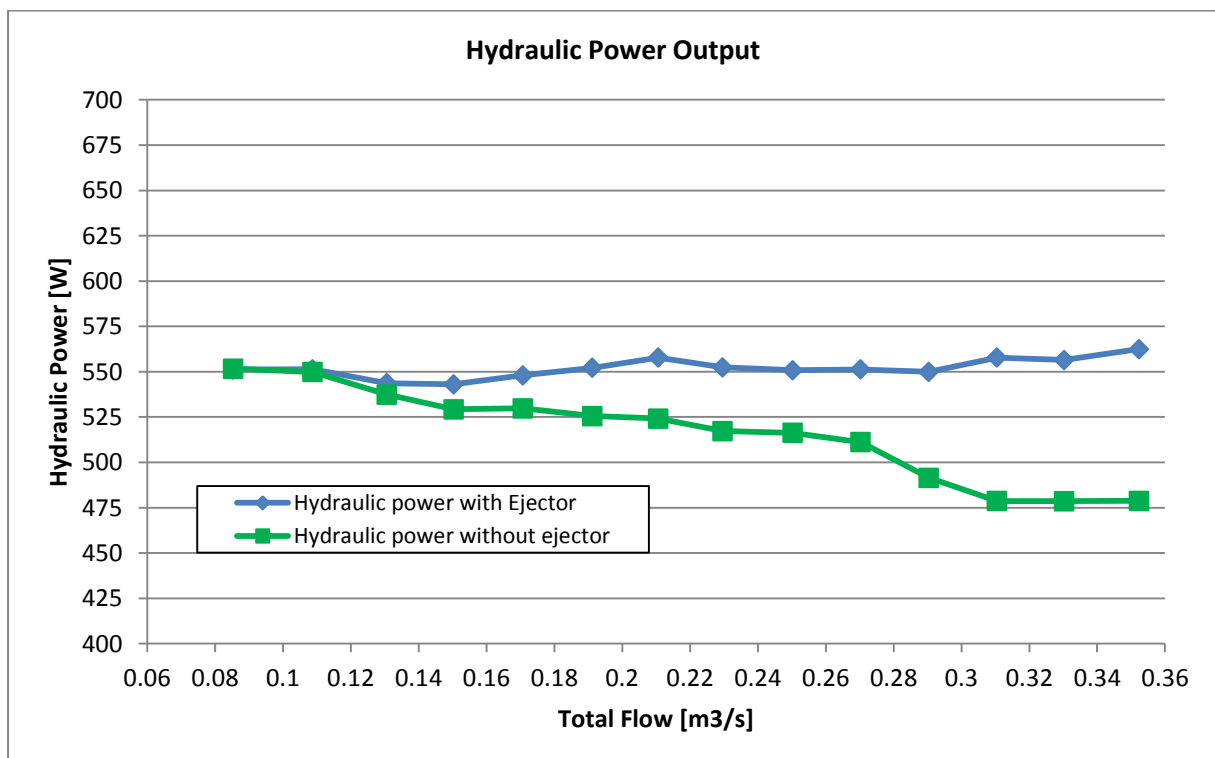


Figure 20. Hydraulic power output with initial tail water level 60 mm above the tip nose.

According to the results seen in figure 20, we have that the hydraulic power with ejector is once again higher than the one calculated for the case without ejector. This again results in a positive effect of the ejector ramp as an increaser of hydraulic power.

### 2.2.5 Tail water level 80 millimeters above the tip nose of the ejector ramp

Figure 21 shows the main characteristics measured for this case. This figure shows that the tailwater level increases from 0.08 meters to around 0.14 meters at the maximum total flow tested. In this figure it is also possible to see that the turbine flow with ejector is again lower than the turbine flow rate without ejector.
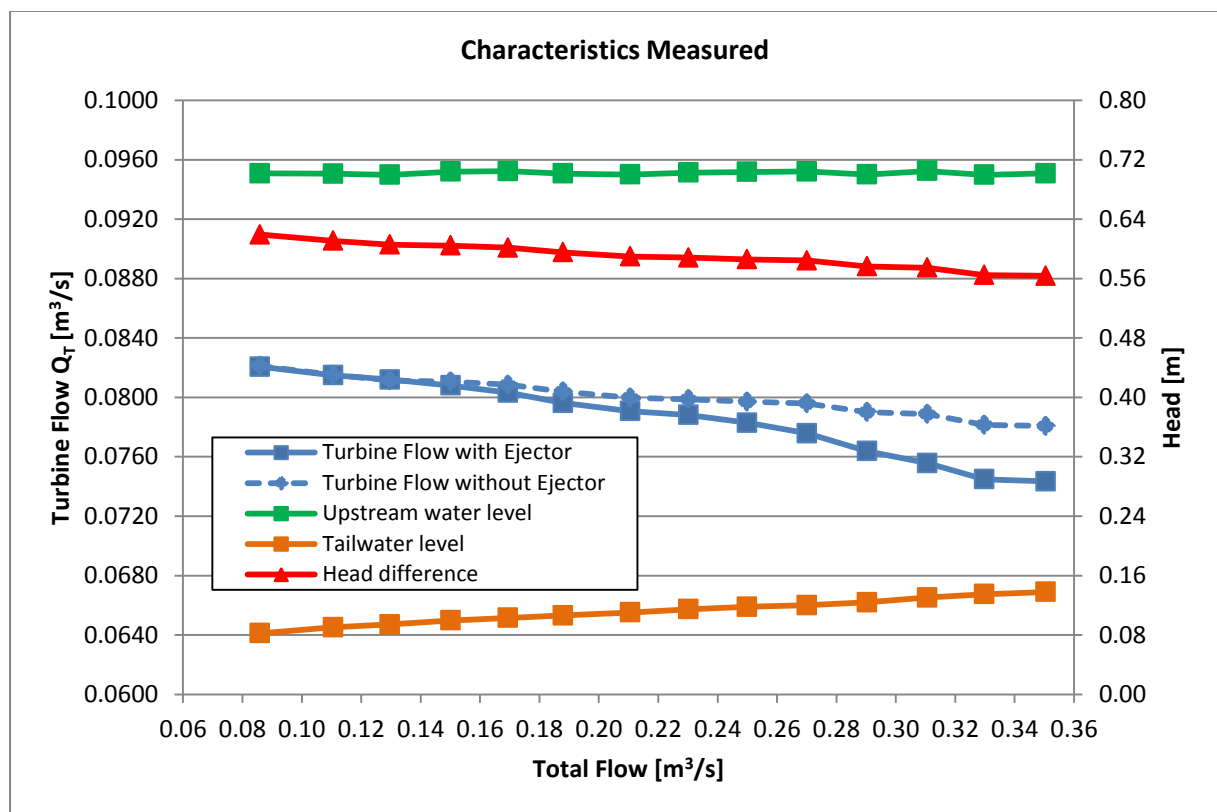


Figure 21. Characteristics measured with initial tail water level 80 mm above the tip nose.

Figure 22 shows the water drop height with ejector and the calculated water drop height without ejector. As in the previous cases, the water drop height is higher when the ejector ramp in implemented and the pressure difference ΔP1 decreases with increasing total flow rate.

Figure 23 shows the results obtained for the hydraulic power in this case.
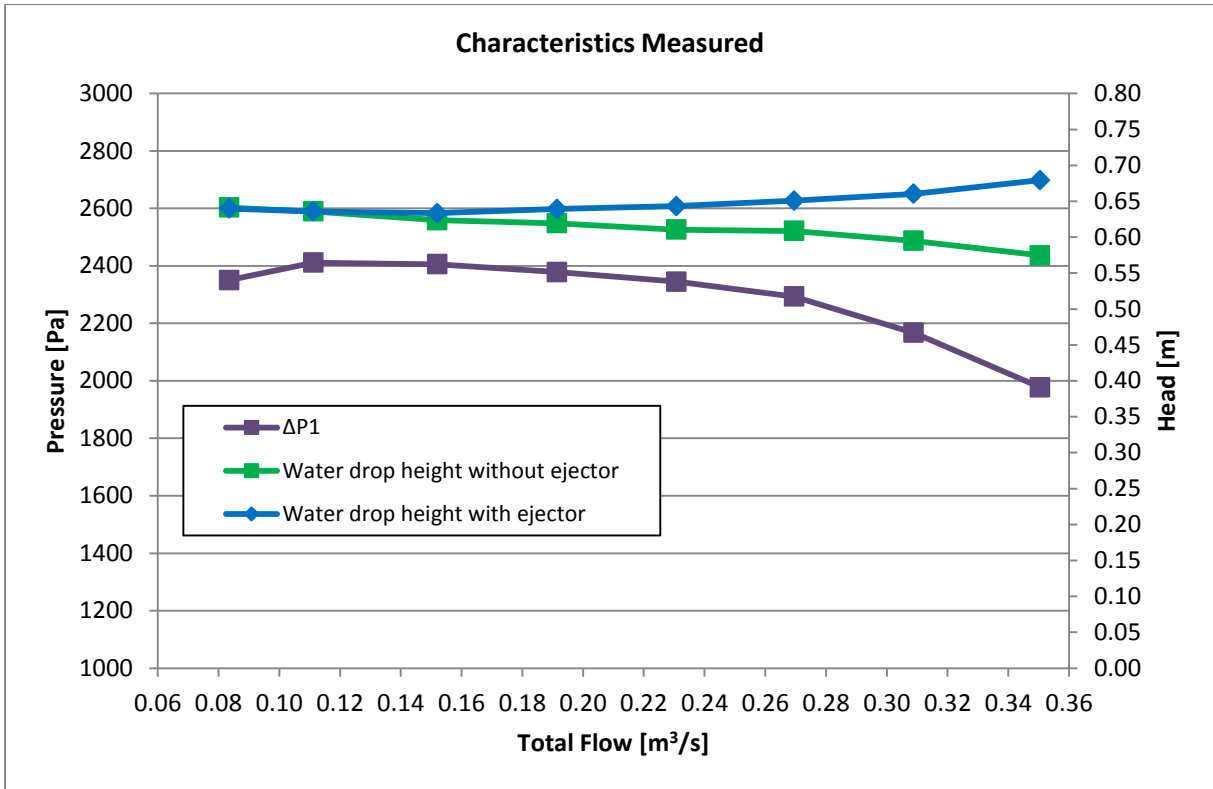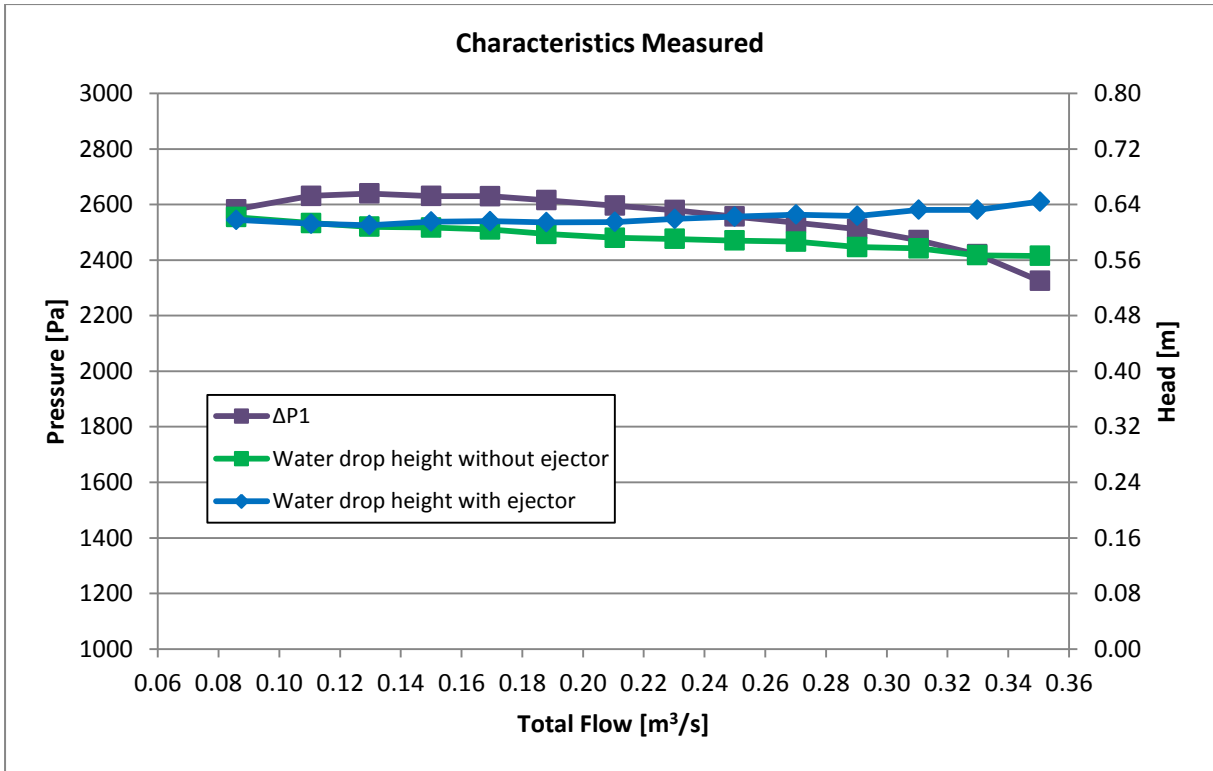
Figure 22. Characteristics measured with initial tail water level 80 mm above the tip nose.



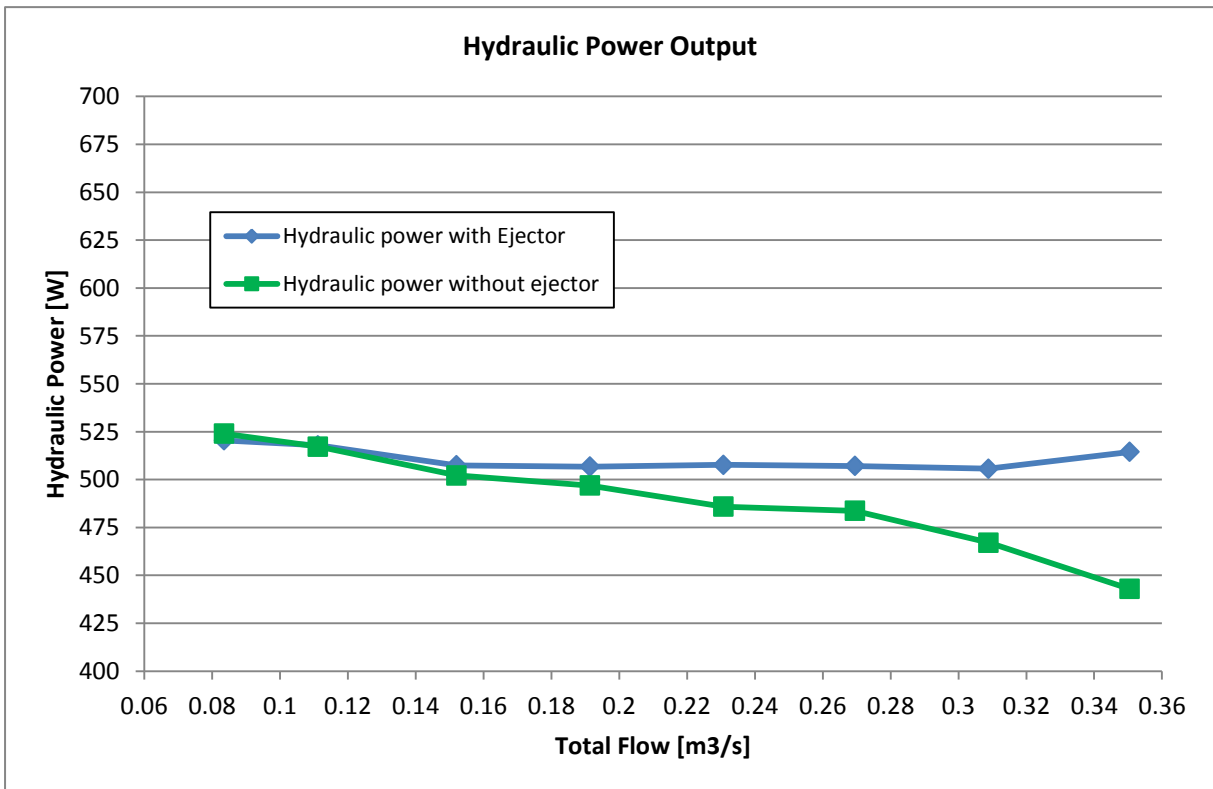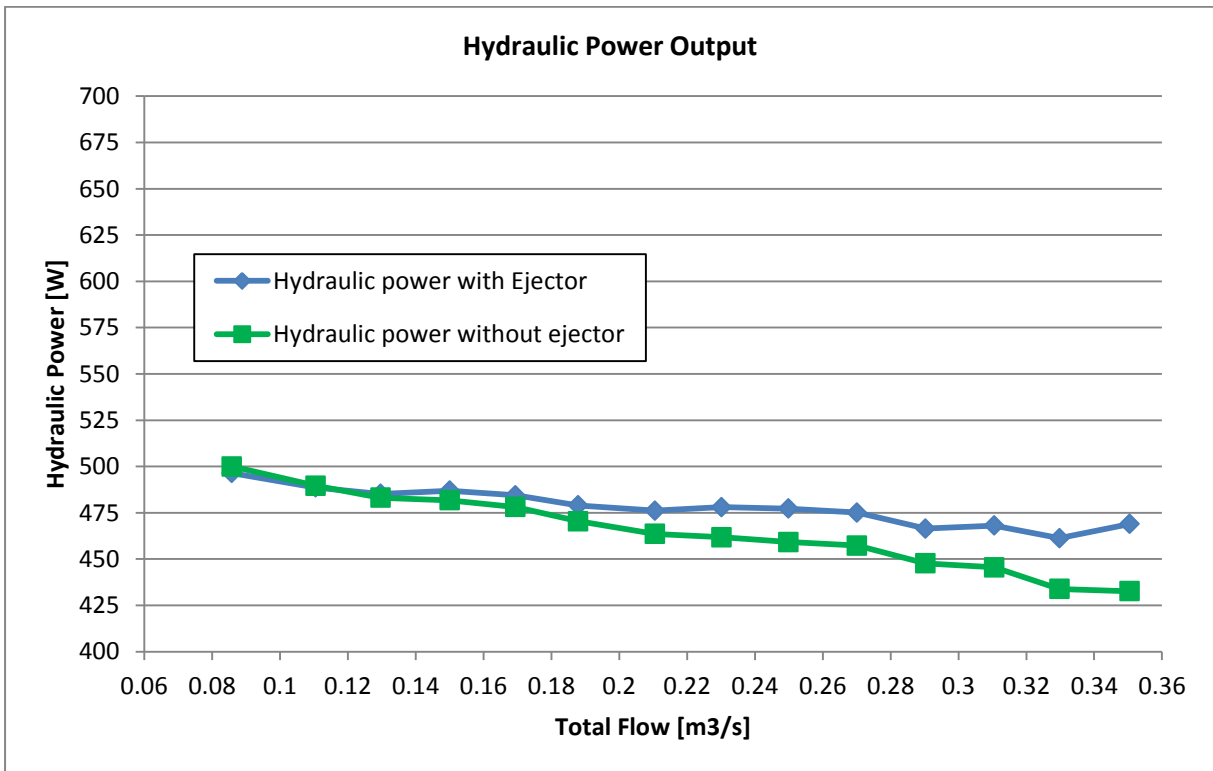Figure 23. Hydraulic power output with initial tail water level 80 mm above the tip nose.

In figure 23 it is possible to see that the hydraulic power with ejector is once again higher than the one calculated for the case without ejector. This again results in a positive effect of the ejector ramp as an increaser of hydraulic power.

## 2.3 EXPERIMENTAL RESULTS ANALYSIS

Since different initial tailwater levels were experimentally tested, it is necessary to compare these results in order to get a better understanding of the working characteristic of the ejector ramp. Figure 24 shows a comparison between numerical results for the different initial tailwater levels studied. This figure shows the average hydraulic power and also the average ΔP1 in each of the cases.
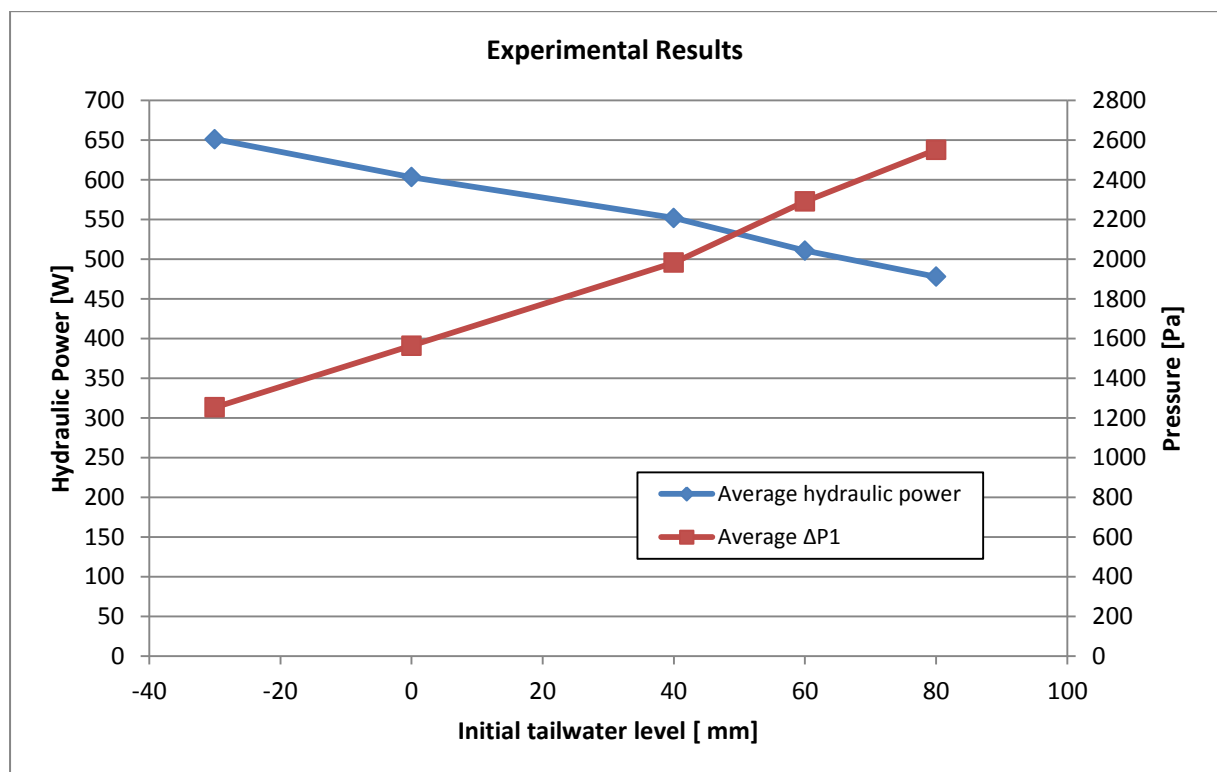


Figure 24. Comparison of experimental results.

In this figure we can see that the higher average hydraulic power is obtained at the lower initial tailwater analyzed. According to the slope of this line, we can conclude that higher initial tailwater levels have a negative impact on the hydraulic power output of the power plant when the ejector ramp is implemented. This result is expected because with higher initial amount of water on the ejector ramp, the water jump is lower and therefore the lowest point of the wake in the mixing zone acquires a new location. This new position will always have lower value in the $y$ axis and less

increase in the effective head. In the other hand we may think that we should use low initial tailwater levels in order to obtain more hydraulic power outcome. This condition needs to be carefully evaluated in terms of the design conditions of the Kaplan turbine used in the power plant. With and inadequate initial tailwater level we can end up affecting the pressure conditions at the exit of the draft tube and therefore causing cavitation in the turbine. If cavitation occurs, the turbine may get critically damaged and there will be not any positive effect for the power plant.

In terms of the average $\Delta P_1$ we have that it increases at higher tailwater levels. This result makes sense based upon the results shown in the same figure for the average hydraulic power. From the physical principal behind the ejector ramp effect, we have that the decrease in pressure at the exit of the draft tube will increase the flow through the turbine and therefore the hydraulic power output. For this reason we have a strong inverse correlation between these two parameters and therefore valid experimental results.

# 3. NUMERICAL ANALYSIS

In order to compare the results obtained experimentally, a numerical analysis is performed by means of Computational Fluid Dynamics (CFD). The software used in this case to simulate the fluid flow and therefore solve the fluid flow governing equations (Navier-Stokes equations) is Ansys. The package used is CFX, which is well known in the fluids field for its accurate results when dealing with hydraulic and turbomachinery.

The purpose of this analysis is to validate the numerical approach in order to use it as a cost-effective tool to analyze future modification in the geometry of the water district as well as different flow and working conditions.

The numerical analysis is performed in steady state mode. The problem environment consists of a two-phase homogeneous model that comprises air and isothermal water. Free surface will be analyzed using a standard free surface model.

The reference pressure is 0 Pascal and buoyancy is included in the model to consider the effects of gravity in the negative Y-direction. The turbulence model used is k-Epsilon with scalable wall function.

The conditions given above are recommended to solve two-phase models. [3]

## 3.1 BOUNDARY AND OPERATING CONDITIONS

The geometry consists on a real-scale representation of the water volume enclosed in the existing district. The height of the water volume is constant at 1200 millimeters along the entire volume. The reason for this is to have 700 millimeters of water above the tip nose of the ejector ramp in the inlet tank. This condition is kept this way so that the simulations are carried out with the same upstream water level as in the experiments and therefore the results can be comparable. For the case of the ejector ramp and the outlet tank where the water does not have this height, it is necessary to impose adequate boundary conditions to solve the problem and to allow the location of the free surface to be an implicit solution of the simulation. The water volume and the boundary conditions used in the numerical analysis to solve the problem are shown in Figure 25.
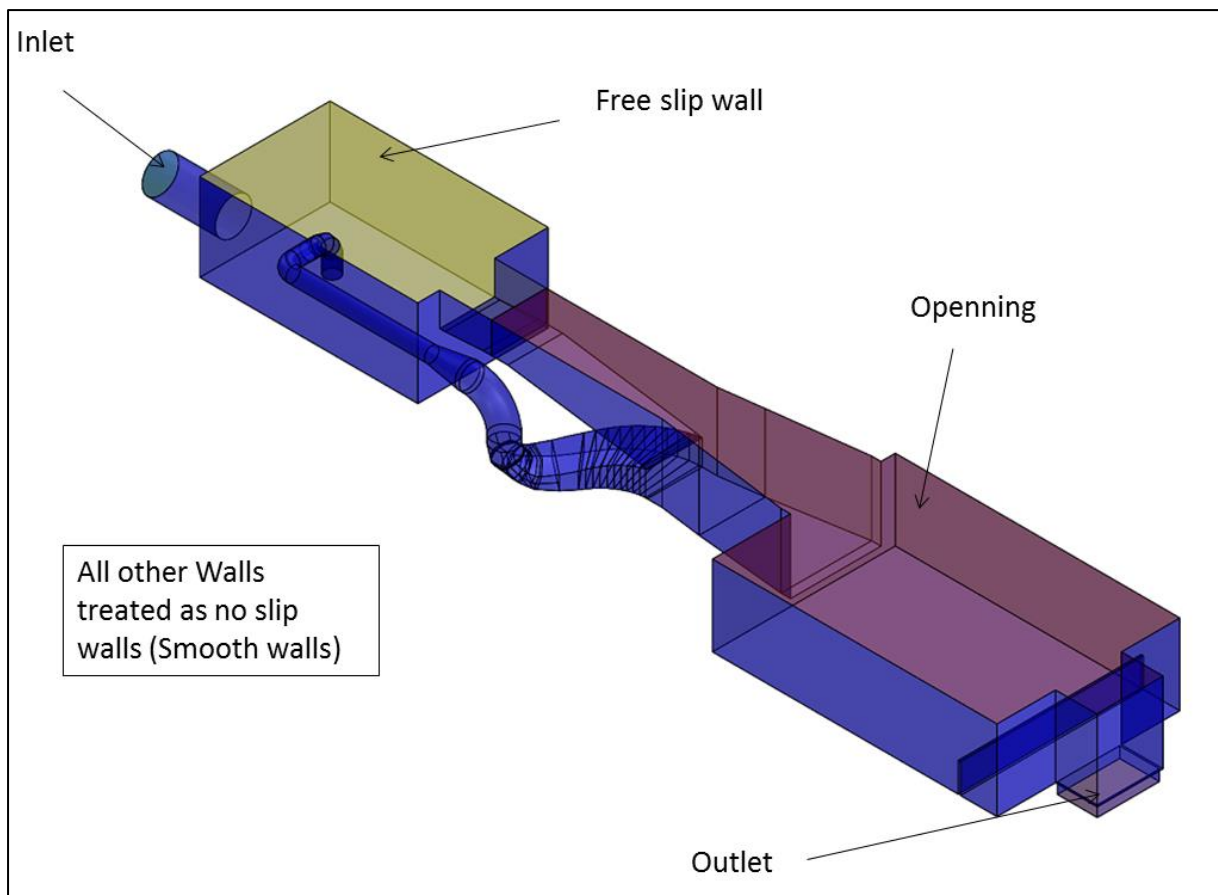
Figure 25. Water volume and boundary conditions for CFD modelling.

Since the model requires the simulation of free surface flows, it is also required to define adequate initial conditions to set up appropriate pressure and volume fraction fields. In order to so, expressions using CEL (CFX Expression Language) are created to define these conditions. The expressions created are shown in the following table.

| Name | Definition |
|------|------------|
| DenRef | *1.185 [kg m^-3]* |
| DenWater | *997 [kg m^-3]* |
| DenH | *(DenWater-DenRef)* |
| DownVFAir | *if((x>-2.1265[m])&&(y>0.28[m]),1,0)* |
| DownVFWater | *(1-UpVFAir)* |

Where *DenRef* is the buoyancy reference density, *DenWater* is the fluid density, *DenH* is the calculated density of the fluid (water density – buoyancy reference density), *DownVFAir* and

*DownVFWater* are the downstream volume fractions of air and water. As it is seen in the table shown above, the *DownVFAir* is defined as a conditional function. The reason for this is to establish only air in the region to the right and above of the lowest point of the ejector gate. This is why this expression is determined based on coordinates along the *x* and *y* directions. These air volume fractions are only used to define the initial condition and are implemented with the objective of facilitating the convergence of the results.

The inlet boundary condition is set as subsonic regime with Bulk mass flow rate defined by the amount of mass flow entering to the system in direction normal to boundary in each different case. This mass flow is set according to the values from the experiments, this again, in order to have results that can be compared. Turbulence intensity at the inlet is established as 5%. Since there is only water entering through this boundary, the volume fraction for the air is set to 0 and the volume fraction for the water is set to 1.

The outlet boundary condition is also set as a subsonic flow regime with average static pressure defined by the mass and momentum option. A relative pressure of 0.03 bar (3000 Pascals) is imposed, which represents an approximation of the height of the water column at the outlet. However, the simulation is not sensitive to the exact outlet fluid height and this approximation is sufficient. It is only used to force the flow downstream and improve the stability of the simulation. The exact height will be calculated as the simulation progresses and therefore this approximation does not affect the validity of the results. [3]

The wall on top of the inlet tank (shown yellow in Figure 24) is considered as a free slip wall. This is due to the consideration of this wall representing the free surface in the inlet tank. Therefore, the water is free to move without any external resistance. The wall on top of the ejector ramp and the outlet basin (shown red in Figure 25) is treated as an opening boundary type. The mass and momentum option is selected as entrainment with relative pressure of 0 bars. The turbulence option is set as zero gradient since it is recommended for this boundary type [3]. Since it is expected to have only air in this boundary wall, the volume fraction of air is set to 1 and the one for water is set to 0.

All other walls, where water touches a solid surface, are considered smooth walls with no-slip condition.

The advection scheme used for the simulation is high resolution and the turbulence model is solved using first order schemes. The convergence criterion for the simulation is based on the residuals of each of the governing Navier-Stokes equations with a residual target of $1\times10^{-5}$. The number of

iteration performed is 750. However, the convergence criterion for the simulations performed in this study is based on the convergence of monitoring points located in region where air or water is expected. Based on the trend of this points the model was selected as accurate or not.

## 3.2 MESHING STRATEGY

The meshing strategy used consists in creating a body of influence in the zone where the free surface zone is expected according to the experimental results. The objective of this body of influence is to include more grid points (nodes) in this zone and therefore increase the resolution and solve with more precision the exact location of the free surface. Figure 26 shows the location of the body of influence in the computational domain.
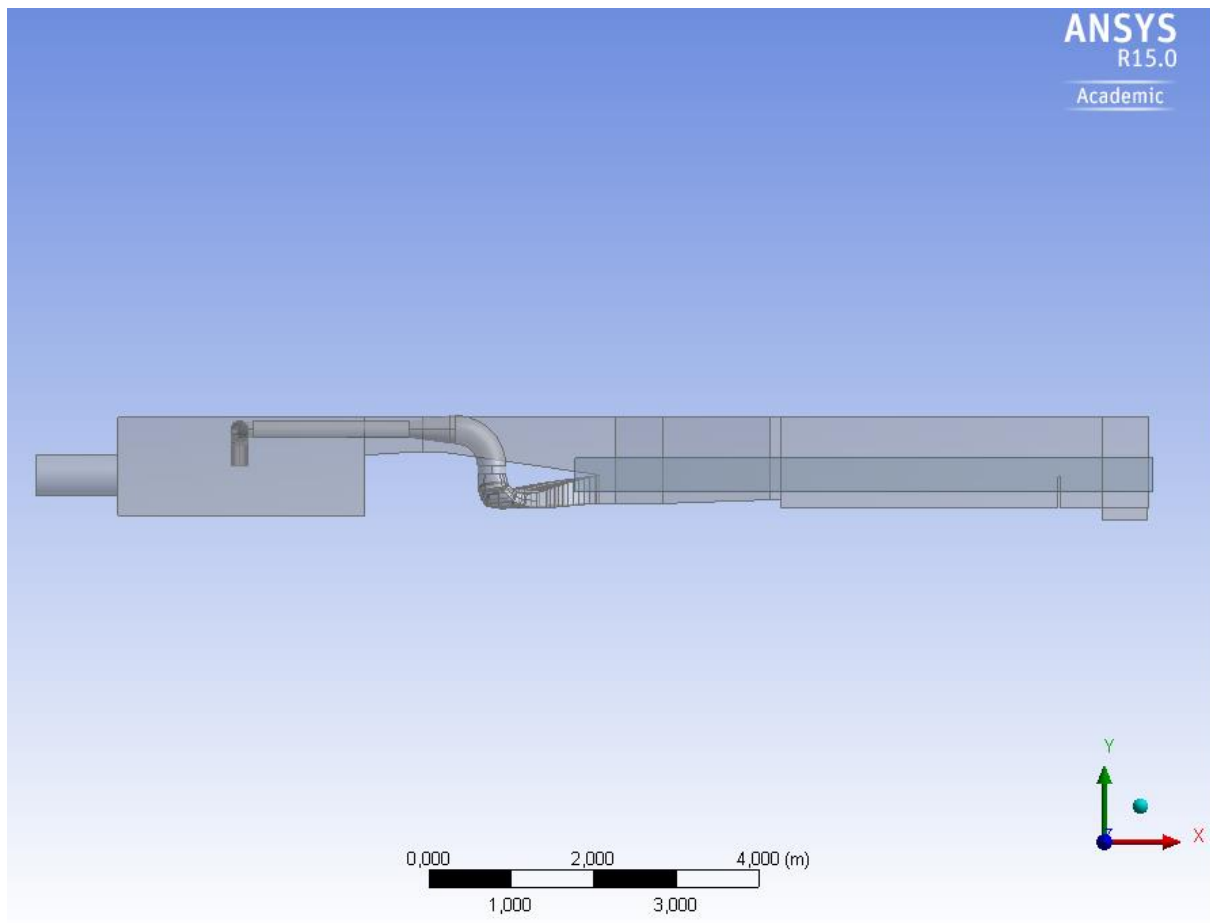


Figure 26. Body of influence in the computational domain.

An inflation layer was created for all the walls with no-slip condition in order to solve with more precision the boundary layer and to consider in the model the effects of the flow separation phenomena. The inflation consists of multiple layers (in this case 8) where the first layer thickness is

equal to 0.5 millimeters with a growth rate among layers of 1.3. Figure 27 shows a zoomed view from the positive Z-direction of the area around the tip of the ejector ramp together with the mesh and the body of influence.
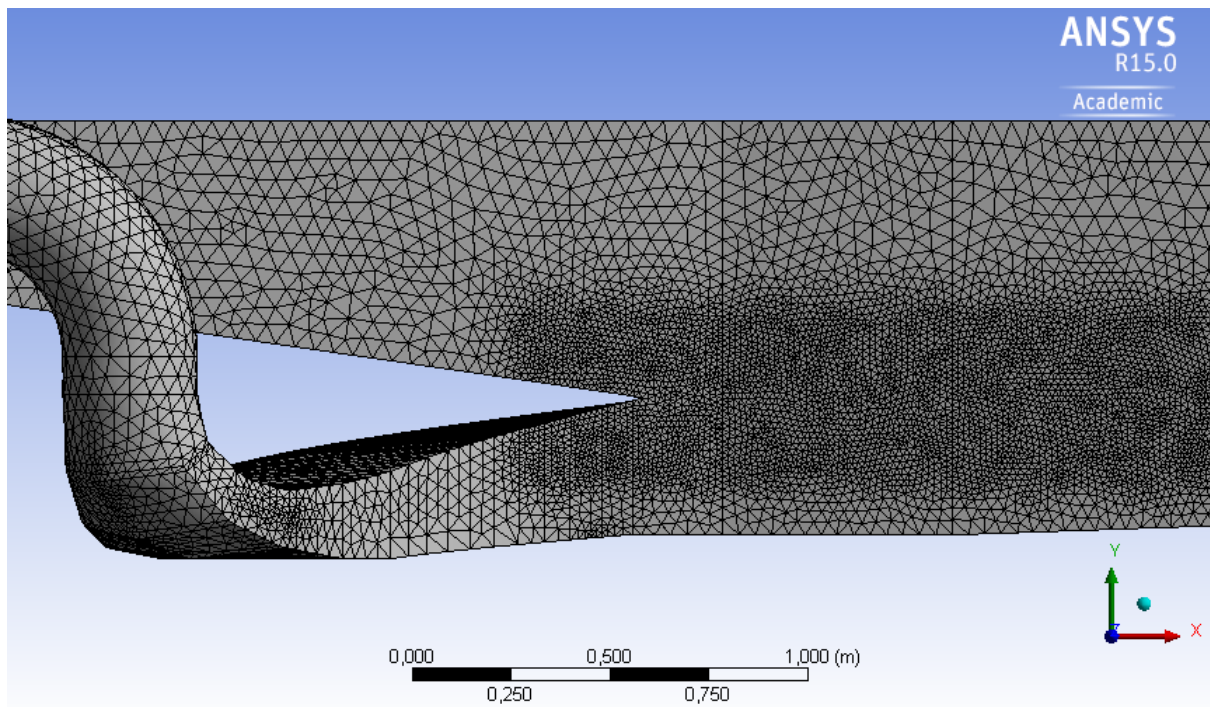


Figure 27. Meshing strategy around tip nose.

In this figure we can see how the body of influence generates finer elements where desired. This methodology allow the implementation of fine elements where interesting phenomena is occurring and coarse element where it is not. This is useful especially to decrease the amount of nodes in the simulation and therefore decrease the overall computation time without sacrificing accuracy in the results.

## 3.3   NUMERICAL RESULTS

### 3.3.1   Ejector gate closed

The first numerical analysis is performed for the case with the ejector gate closed, thus no water is flowing down the ejector ramp. In this case the maximum element size for the global mesh is 50 millimeters and the maximum element size within the body of influence is 15 millimeters. The resulting mesh consists of 3,226,608 nodes and 16,625,999 elements. For this case the inlet

boundary condition is set to a mass flow rate of 88.73 kg/s, which correspond to the average 89 lit/s that the pump is delivering to keep the upstream water level constant at 700 millimeters as it was in the corresponding experimental case. The visualization of the results will be carried out using a contour located on a XY-plane that crosses the water volume right in the center ($z = 0$). Figure 28 shows the water volume fraction contour for this case.
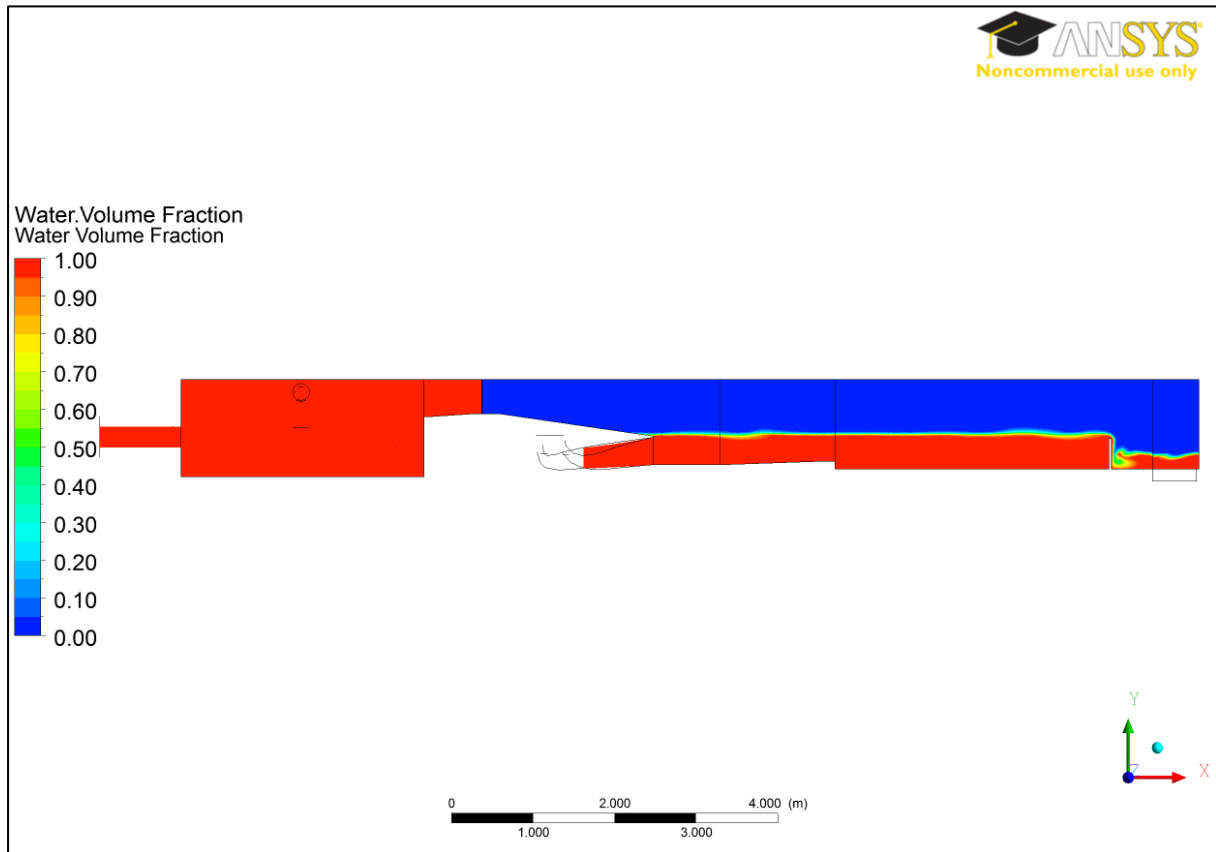


Figure 28. Water volume fraction contour.

In this figure the red color (Water volume fraction equals to 1) means that only water is occupying that volume. As we can also see, the inlet tank is completely red, which is expected according to the definition of the problem where we have that the total height of the water volume corresponds to 700 millimeters head. The blue color (Water volume fraction equals to 0) means that only air is present. We can see that in the ejector ramp and in the outlet tank, the top portion is completely blue, which also agrees with the expected condition. In accordance with the experimental analysis, when the ejector gate is closed the free surface should be located right at the tip nose of the ramp. Figure 29 shows a closer view into the ejector ramp tip nose area and figure 30 shows a closer view of the region after the wooden weir.

Figure 29. Water volume fraction at the tip nose of the ejector ramp



Figure 30. Wake region as water passes the wooden weir.

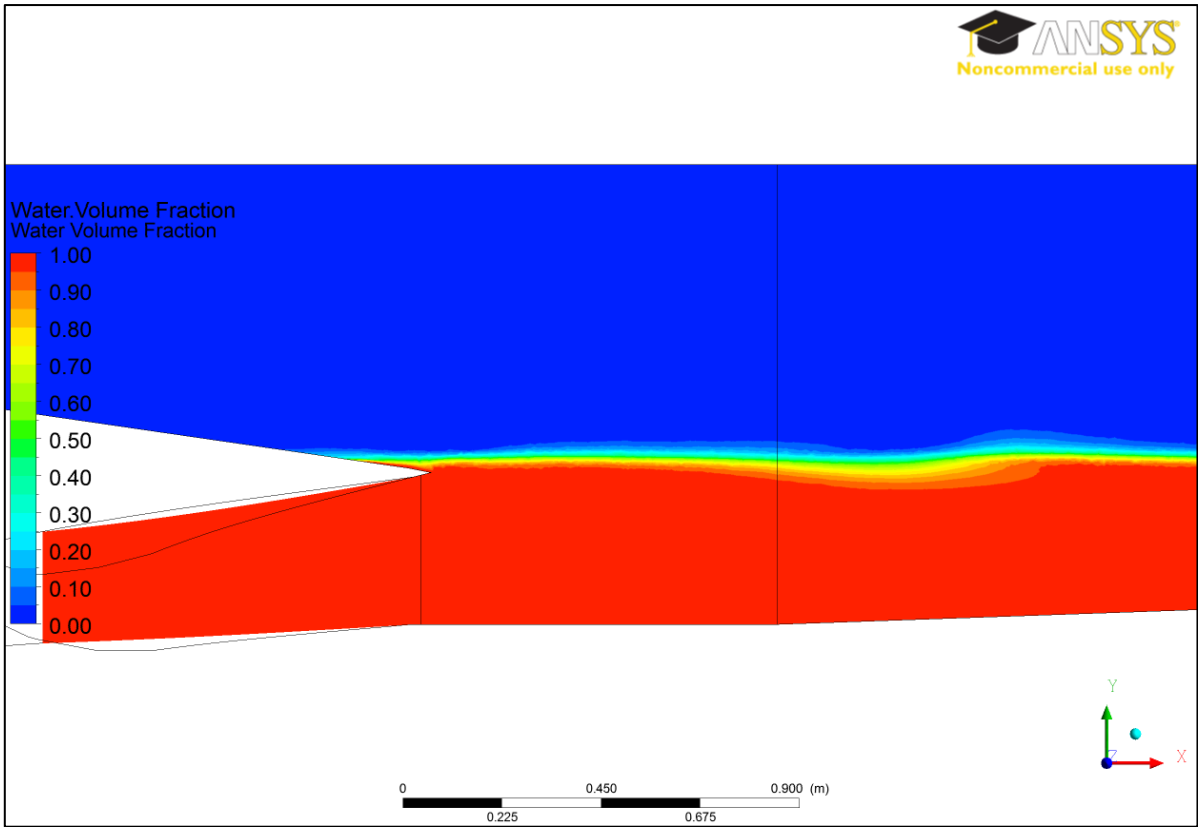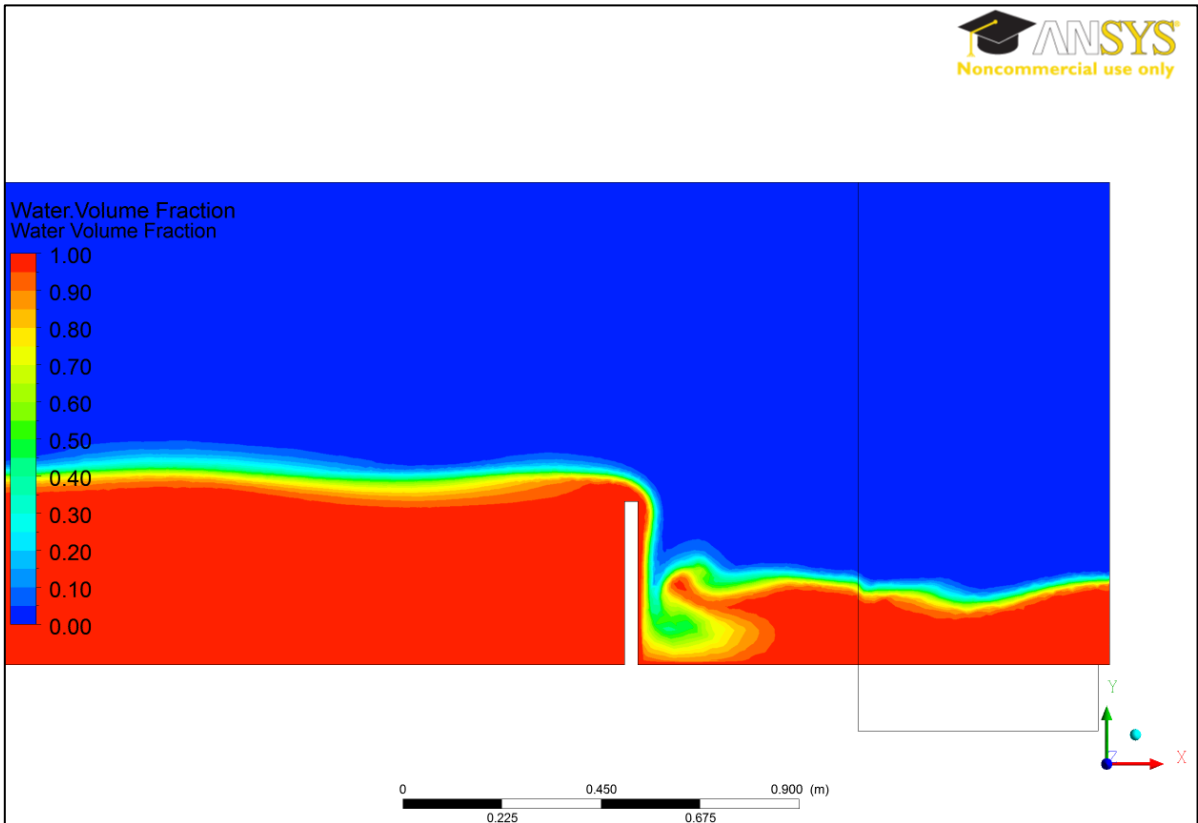In figure 29 it is possible to see that there is a transition from having only water at the bottom to having only air at the top. This transition corresponds to the free surface. In this case we can see that the free surface is located right at the tip nose as expected from experimental results.

In Figure 30 we can see that once the water passes the weir forms a wake that is conformed of water and air mixed and looks like a recirculation zone due to the water jump. This situation is also seen in the experimental test and helps to visually confirm the validity of the simulation.

This figure also shows that the height of the water column right at the outlet is not equal to the one imposed in the outlet boundary condition. This height is computed and adjusted as the simulation progresses. As a second step to validate the numerical results, a pressure contour is created in the same plane that was used before and it is shown in Figure 31 in the inlet tank.
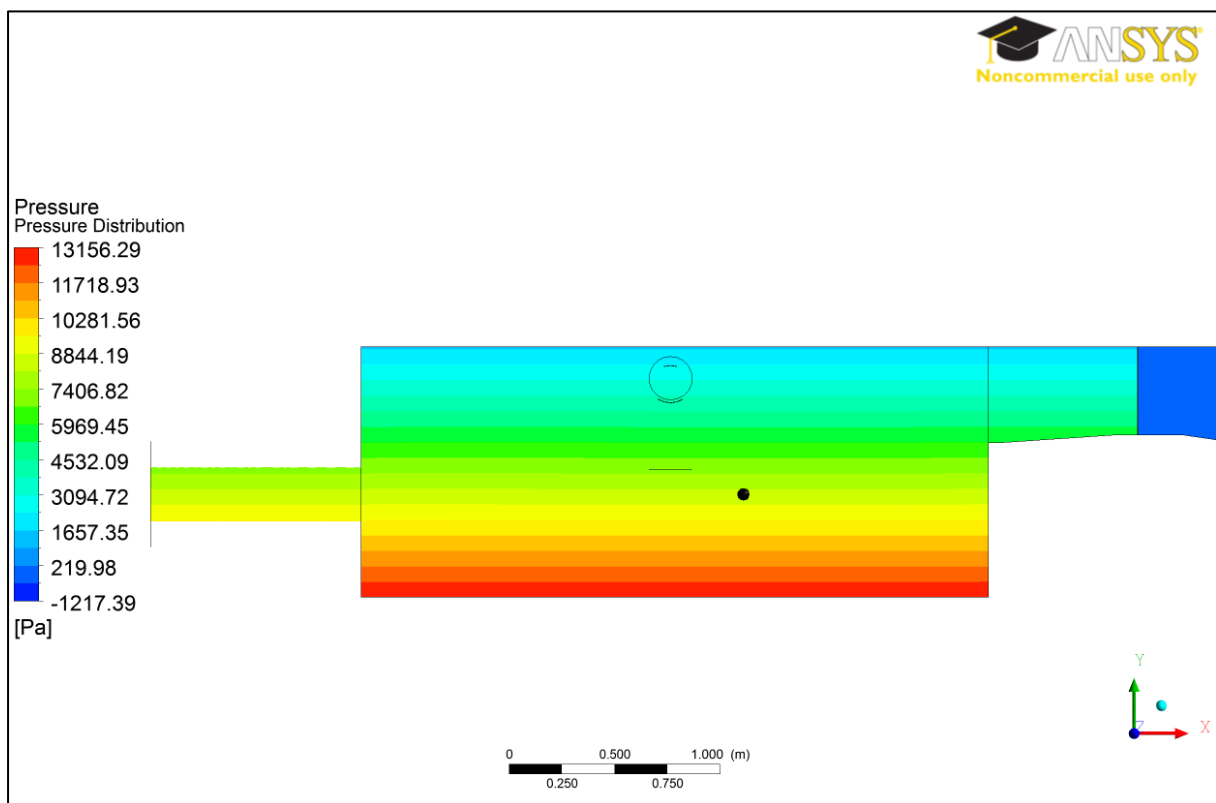


Figure 31. Pressure distribution in the inlet tank with ejector gate closed.

The inlet tank is the especial interest in terms of pressure. In figure 31 it is seen a dark point in the contour. This point is located at the same height as the tip nose ($y = 0$) which means that there is 700 millimeters column of water above this point. The objective of this is to compute the pressure and compare it with the one theoretically expected. With a water column of about 0.7 meters, the static pressure should be around 7000 Pascals. Evaluating the pressure at the dark point in figure 30 we have a value of 8360.63 Pascals. Although there is a difference in terms of pressure, the

simulation still shows good agreement with real conditions. For this reason, this procedure will be adopted to perform the simulations with ejector gate opened. The discrepancies in terms of pressure are left to the end to analyze its overall effect in the final results.

### 3.3.2 Ejector gate opened

For the simulations when the ejector gate is opened, only the case when the tail water level is located at the tip nose will be considered. The parameter that will be changed is the inlet boundary condition (mass flow rate at the inlet). The reason for this is the high number of nodes in the model, which complicates the simulation taking approximately 60 to 72 hours to get solved using a high-performance computer (64 Gigabytes memory ram and 16-core processor).

The meshing strategy in this case is the same as before. The only difference is that the body of influence is modified to include more elements into the ejector ramp and the area of aperture of the gate to accurately calculate the amount of water and velocity at which it is flowing through the ramp. Figure 32 shows the modification done to the body of influence.
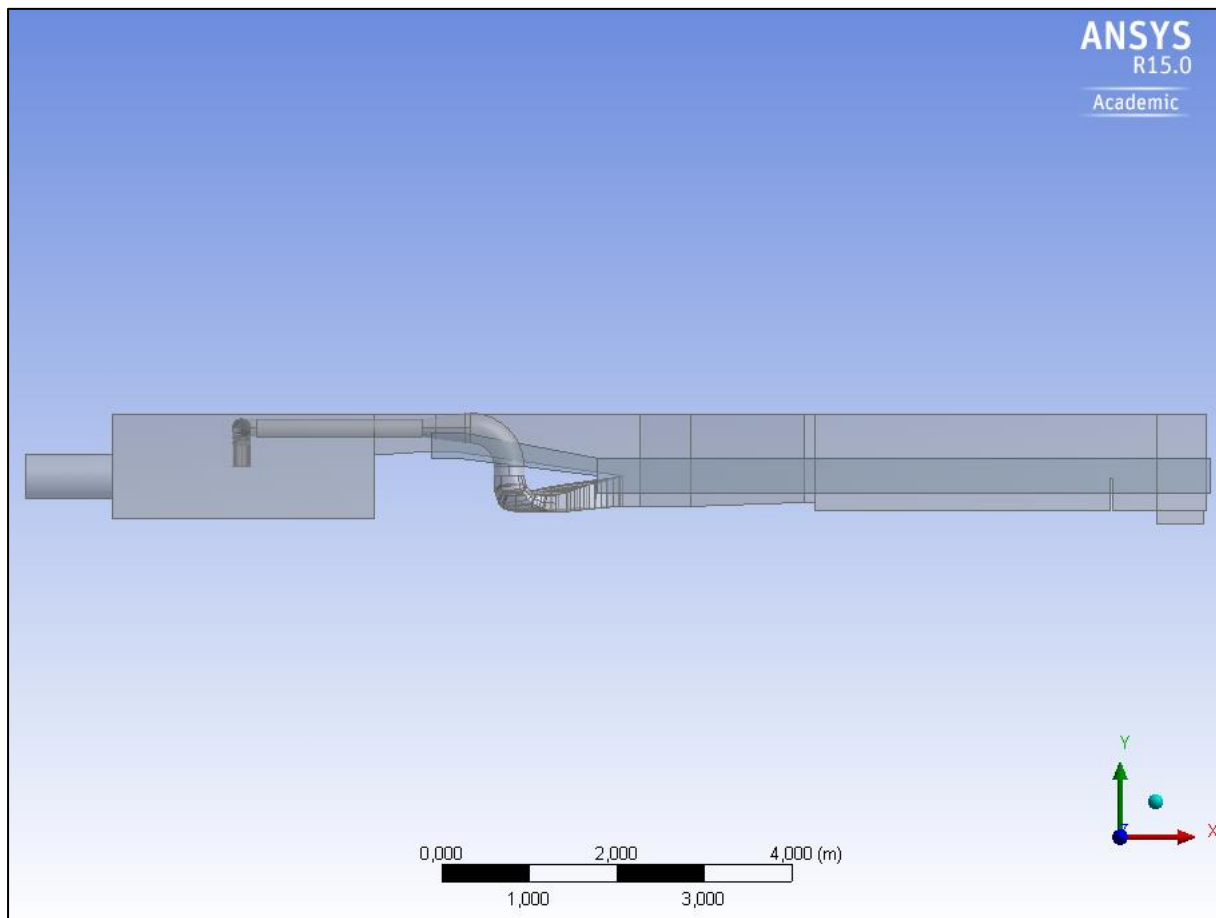


Figure 32. Body of influence in the computational domain when ejector gate is opened.

Figure 33 shows the resulting mesh after applying the body of influence into the water volume.
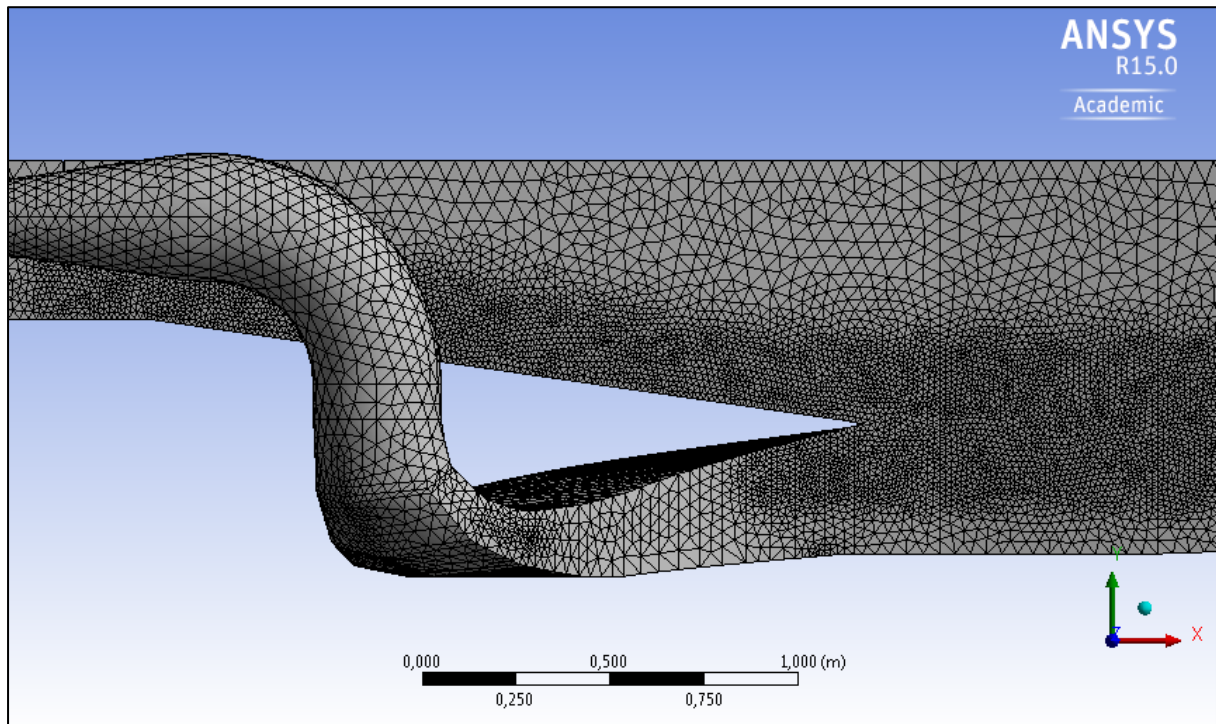


Figure 33. Meshing strategy around tip nose and ejector ramp.

As in the previous case, we can see in figure 33 that finer mesh is included in the area where the free surface is expected as well as in the ejector ramp.

### 3.3.2.1    Flow rate: 130 lit/s.

This case involves an inlet boundary condition of 129.61 Kg/s. The ejector gate now needs to be opened to allow water to flow down the ramp. The aperture of the gate is taken from the corresponding experimental case. This aperture was measure and set to 30 millimeters, this in order to keep the upstream water level constant. Figure 34 shows the water volume fraction for this case. In this figure we can see that now there is water flowing down the ramp and there is a wake region formed after the ejector ramp due to the mix of flow coming from the draft tube and the ramp.

Figure 35 shows a closer view of the ejector ramp and the mixing zone. As expected, the red region (water only) on the ramp is small. This is due to the little aperture given to the ejector gate.
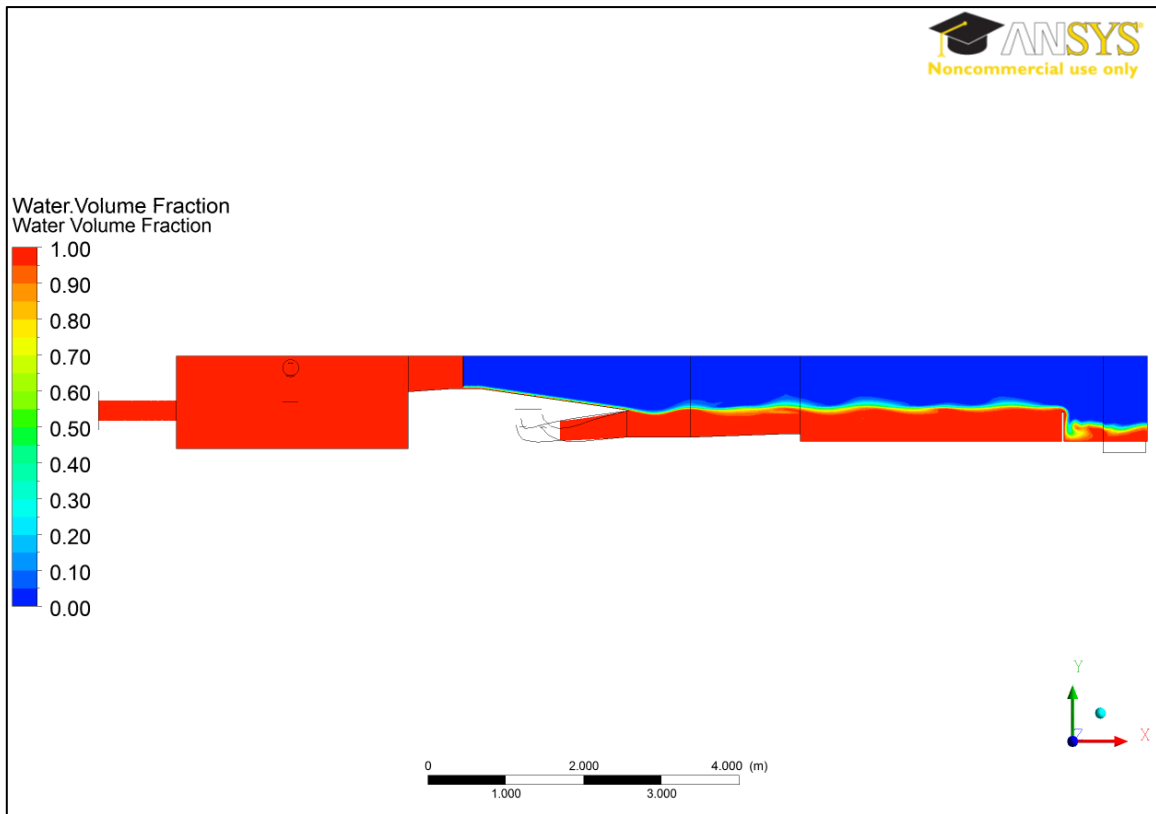
Figure 34. Water volume fraction with gate opened and 130 lit/s inlet flow rate.



Figure 35. Water volume fraction (zoomed view) with 130 lit/s flow rate at the inlet.

35

Figure 36 shows the pressure contour in the inlet tank together with a dark point where the pressure will be measured. This point is located in the same position as it was for the case with the ejector gate closed. The purpose of this is to know how the pressure changes as the inlet boundary condition and the ejector gate aperture change.
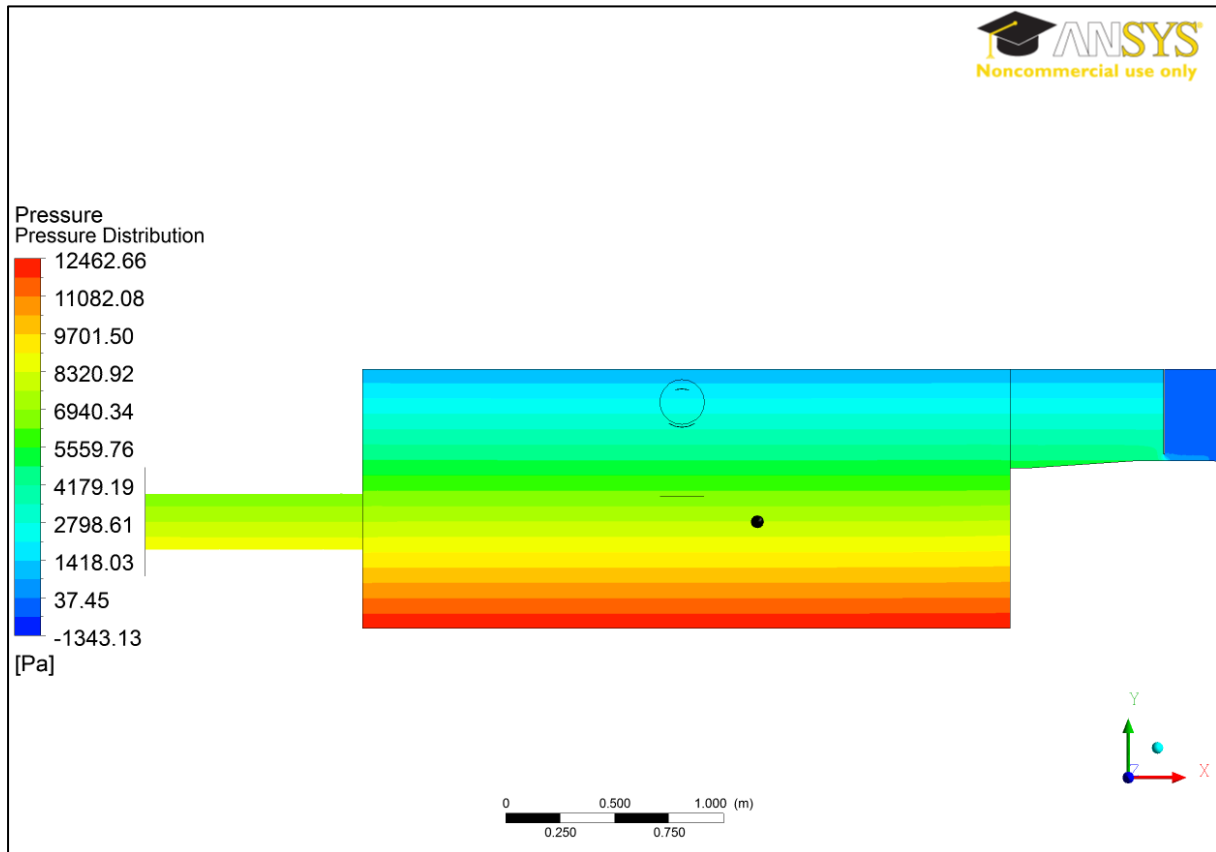


Figure 36. Pressure distribution in the inlet tank with ejector gate opened and 130 lit/s flow rate at the inlet.

As it was explained before, the black point in figure 36 has 700 millimeters of water column on its top since the upstream water level is kept constant. In this case we have a pressure in this point of 7631.54 Pascals, which is closer than the previous case to the expected 7000 Pascals of pressure with this water column.

### 3.3.2.2 Flow rate: 170 lit/s.

In this case an inlet boundary condition of 169.49 Kg/s mass flow rate was imposed. The gate is opened 65 millimeters to allow more water to go down the ramp and keep the upstream water level constant. The water volume fraction for this case is shown in figure 37.
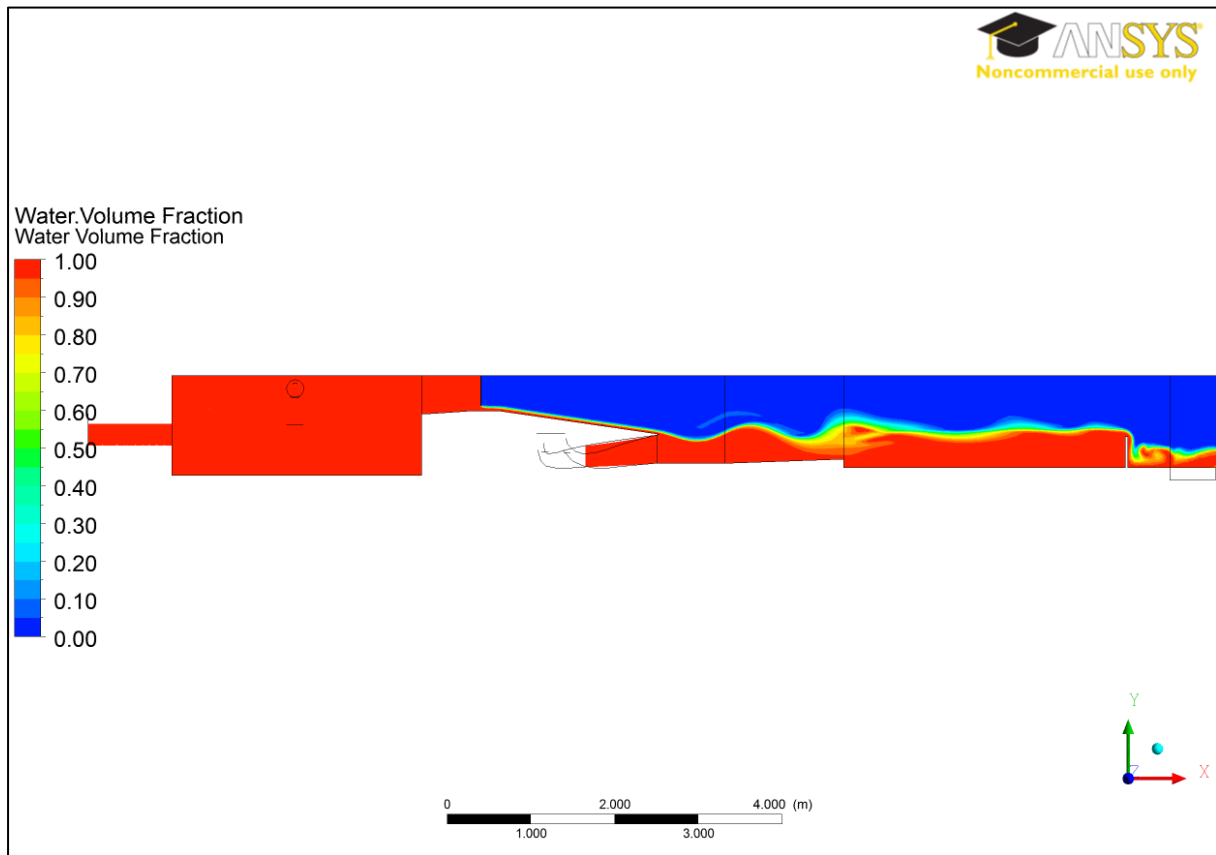


Figure 37. Water volume fraction with gate opened and 170 lit/s inlet flow rate.

For this case, the aperture of the gate is higher than in the previous one and therefore we have more flow rate through the ramp. This can be seen in figure 37 and also in more detail in figure 38. We have that the mix of water generates waves in the mixing zone that are more prominent for this case. This generation of waves is the effect obtained in the experimental tests and therefore confirms that the simulations are giving results that are valid in terms of free surface behavior. A deeper analysis will be carried out later in this text to analyze the validity of these numerical results.

Figure 38 shows the pressure contour in the inlet tank as well as the black point where the pressure is computed. The procedure followed in this case is exactly the same that was used for the previous case.
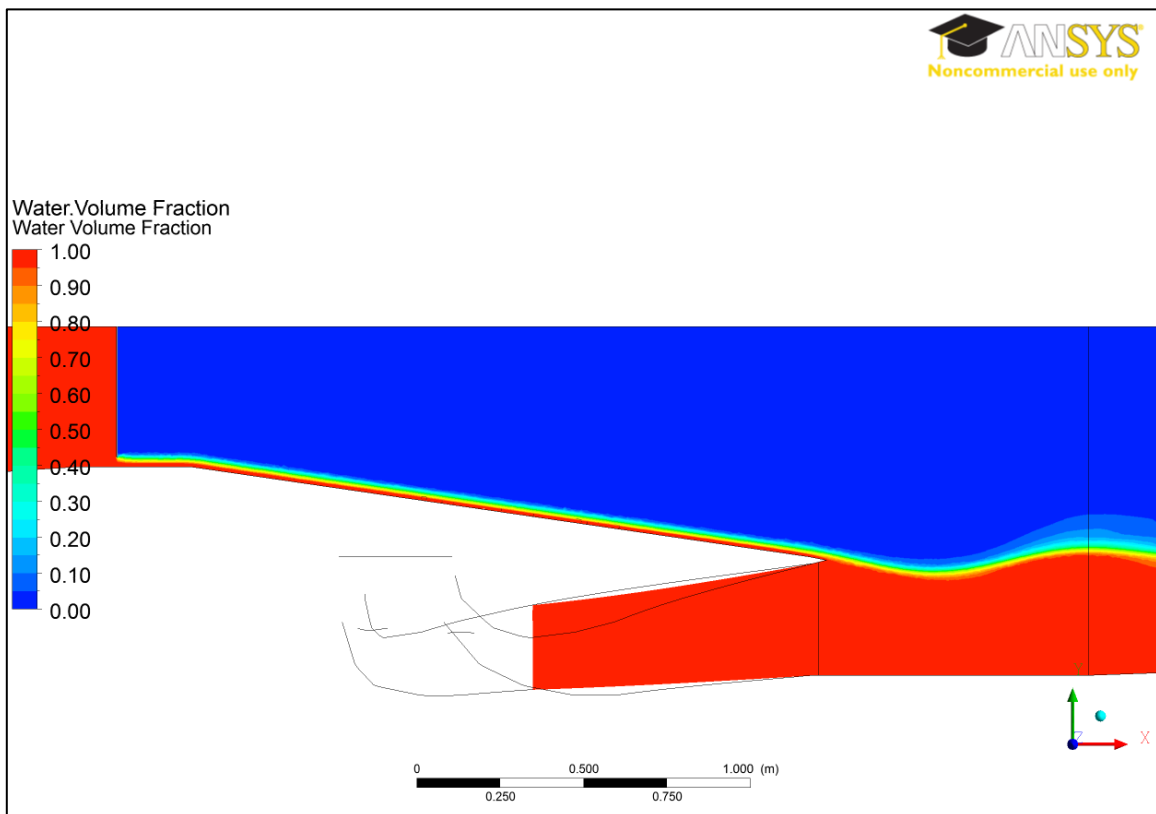
Figure 38. Water volume fraction (zoomed view) with 170 lit/s flow rate at the inlet.
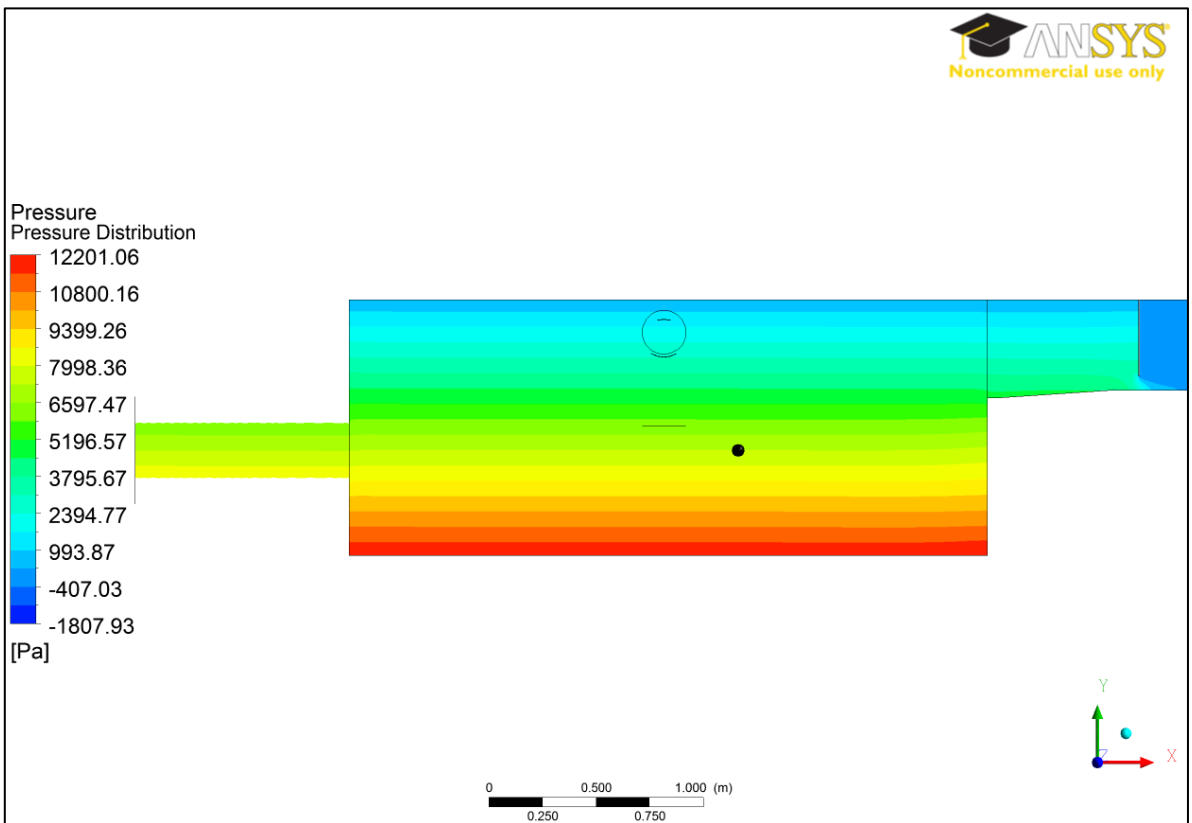


Figure 39. Pressure distribution in the inlet tank with ejector gate opened and 170 lit/s flow rate.

In this case we have that the pressure in the dark point is 7302.54 Pa. This is not exactly the expected value but it does not differ much from it and therefore it is acceptable.

### 3.3.2.3  Flow rate: 210 lit/s.

In this case the ejector gate is opened 99 millimeters and the inlet mass flow rate boundary condition is set to 209.37 kg/s. The water volume fraction contour for this case is shown in figure 40 and a zoomed view is shown in figure 41.
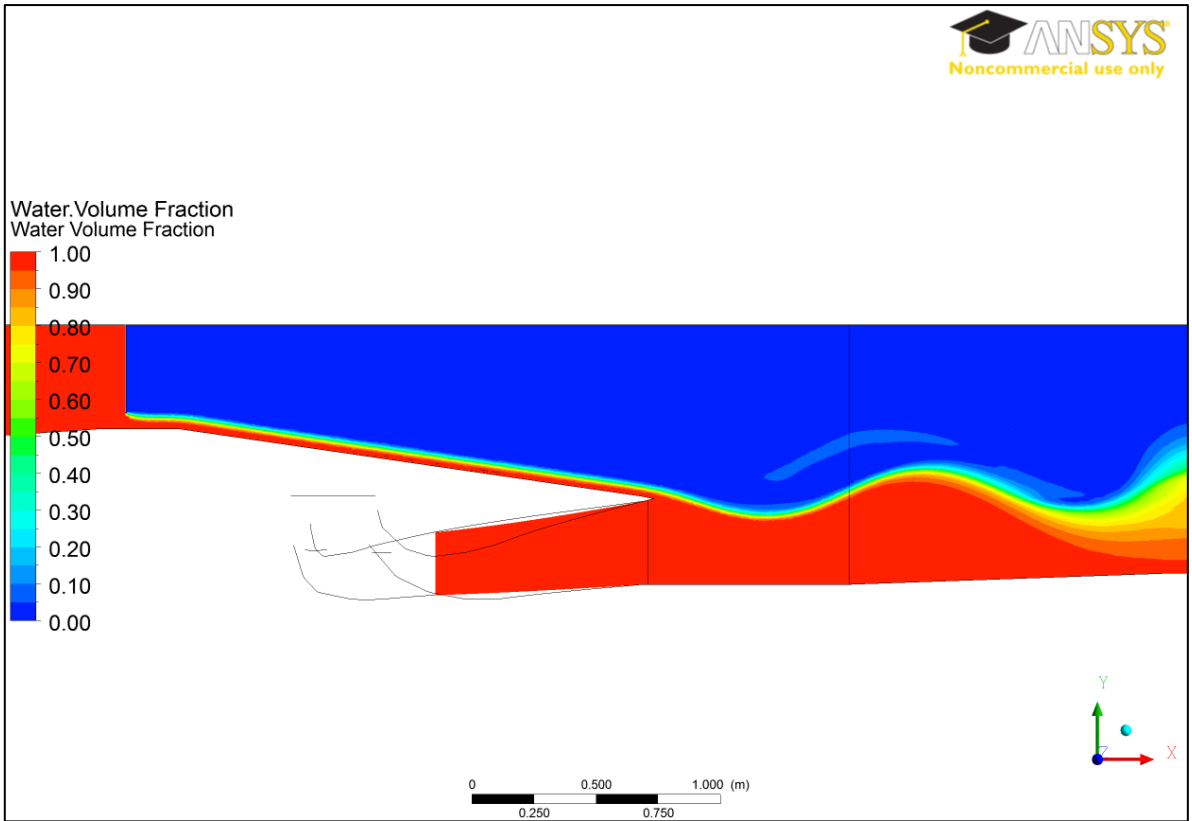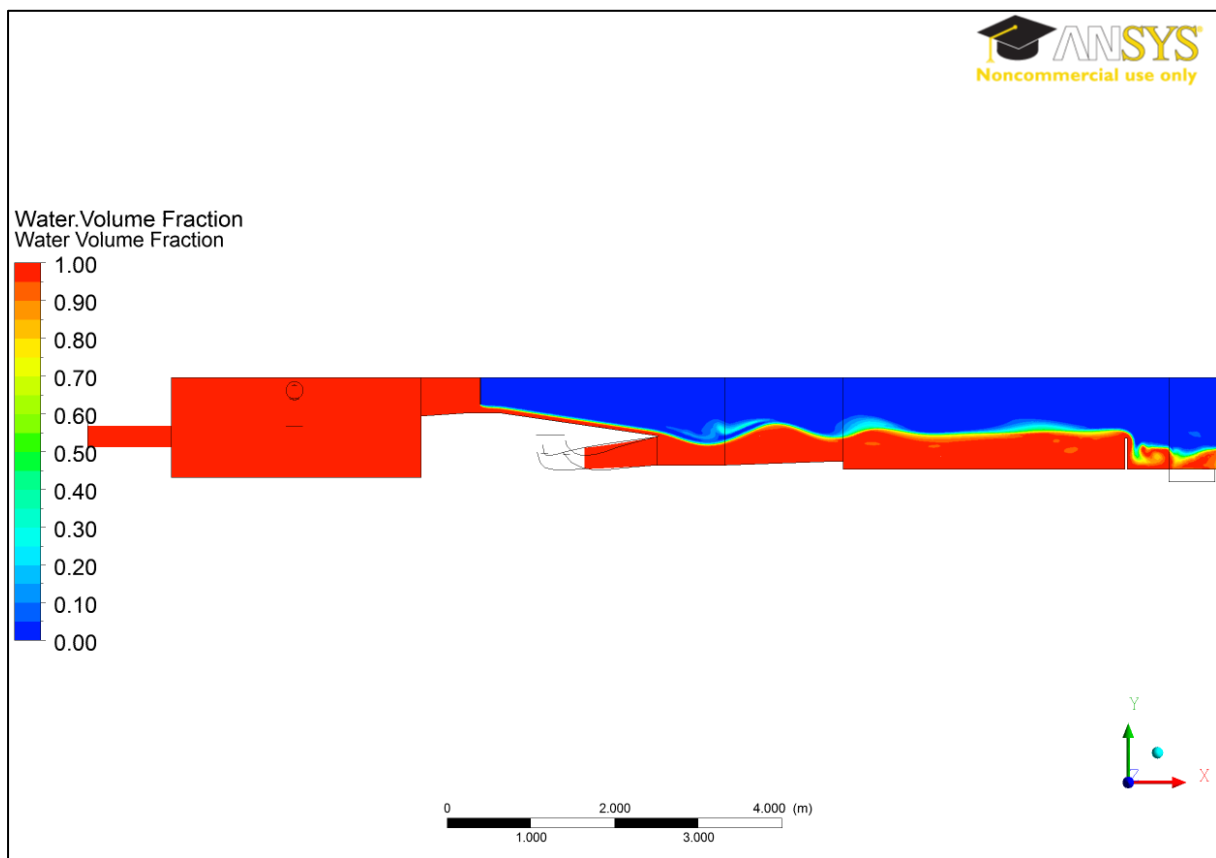


Figure 40. Water volume fraction with gate opened and 210 lit/s inlet flow rate.

As expected, the waves in the mixing zone are stronger in this case compared to the previous one. We can also see in figure 40 that after the weir there is still recirculation zones due to the water jump that become more notorious in every case. In addition, the height of the column of water at the outlet is higher in a small amount compared to the previous cases.

Since the outlet boundary condition is constant for all the models, this result confirms that water column at the outlet is not being affected by the imposition given to this boundary condition. On the

contrary the height of the water column at the outlet is being calculated and is an implicit result of the simulation. Once again we have valid behavior of the free surface compared with the experimental case.
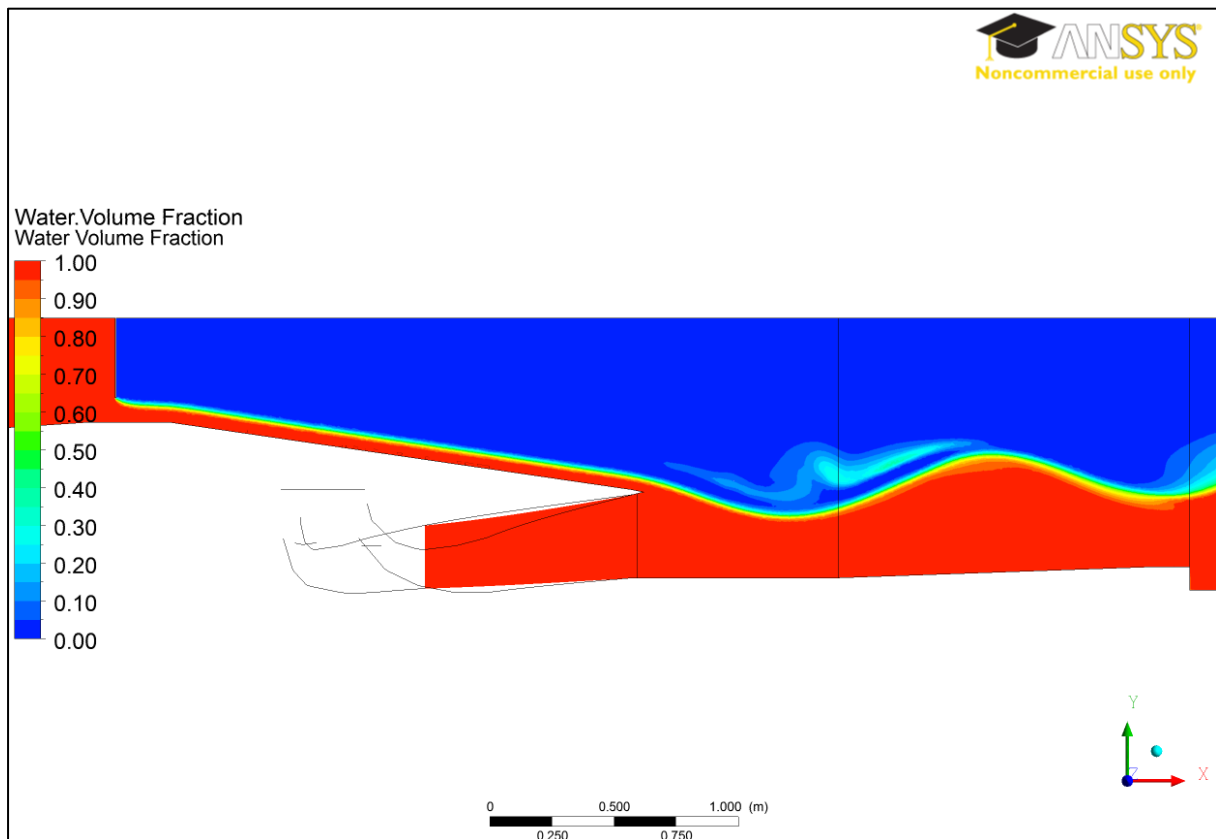


Figure 41. Water volume fraction (zoomed view) with 210 lit/s flow rate at the inlet.

Figure 42 shows the pressure contour in the inlet tank together with the dark point previously used to compute the pressure. In this case we have a pressure in the dark point of 7201.51 Pascals, which is close the expected value and therefore represents an accepted result.

As in can be seen from the results up to this point, the pressure in the dark point in the inlet tank for all the cases is decreasing each time. This variation may be due to the aperture of the ejector gate which is allowing more water to flow down the ramp and leave the tank, releasing pressure from it. However, this assumption will have to be clarified later on when all the results are finally presented and more objective analysis can be carried out.
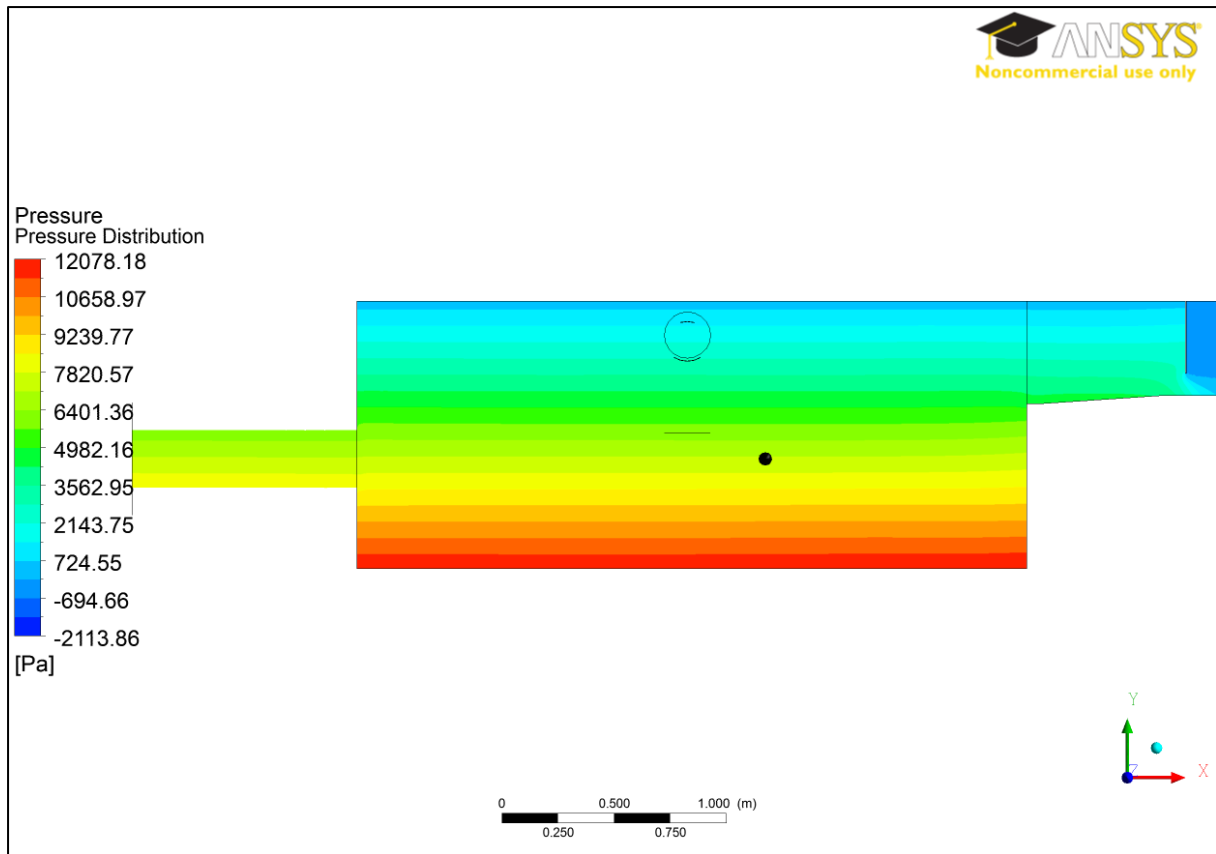
Figure 42. Pressure distribution in the inlet tank with ejector gate opened and 210 lit/s flow rate at the inlet of the tank.

### 3.3.2.4 Flow rate: 250 lit/s.

For this case the inlet mass flow boundary condition is imposed at 249.25 Kg/s with an aperture of 145 millimeters in the ejector gate. The water volume fraction contour for this case is shown in figure 43 and a zoomed view is shown in figure 44.

Once again we can see a strong pattern of waves in the mixing zone. Up to this point the waves have become more prominent as the gate is open wider and more water flows through the ejector ramp. Although a clear comparison of the results has not been done yet, it is possible to use this trend to evaluate the results so far. In this order of ideas we have that this trend directly relates with the behavior seen in the experimental tests. Based upon this we can consider the numerical results to be consistent and therefore can be taken to a deeper analysis later on.
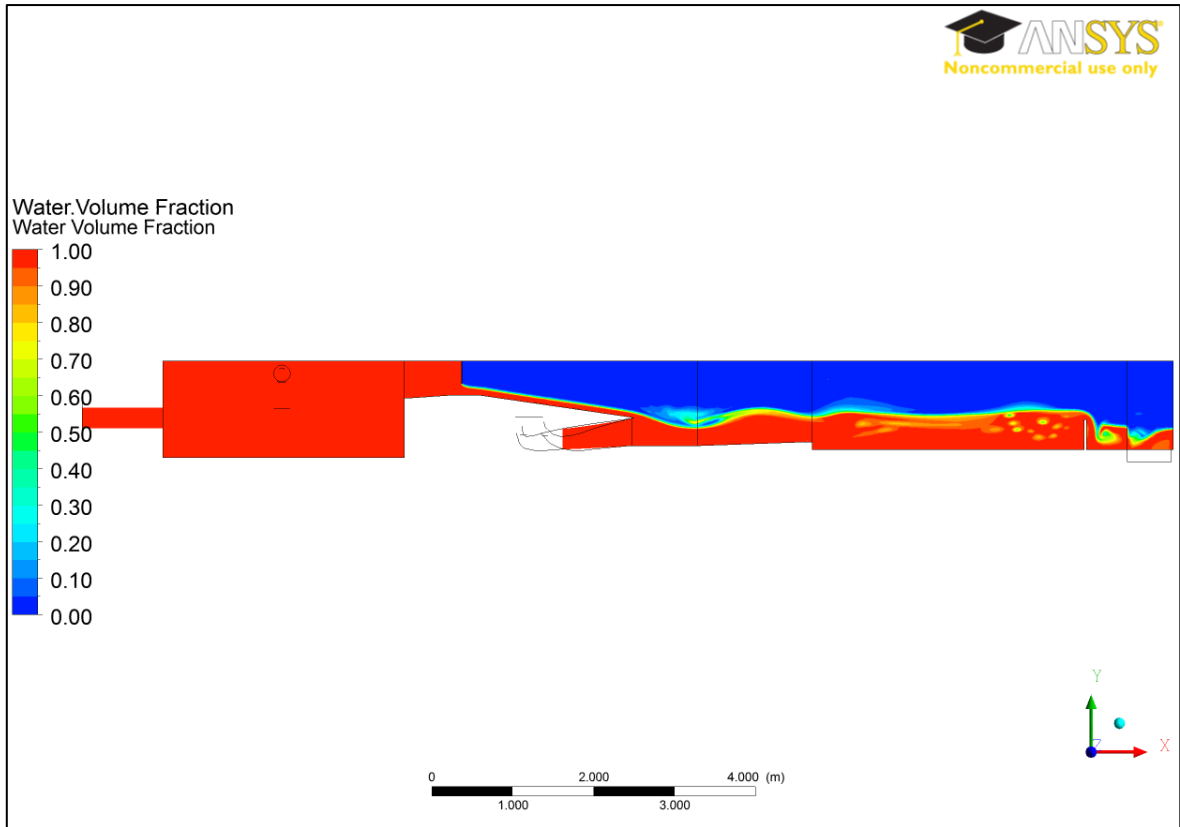
Figure 43. Water volume fraction with gate opened and 250 lit/s inlet flow rate.
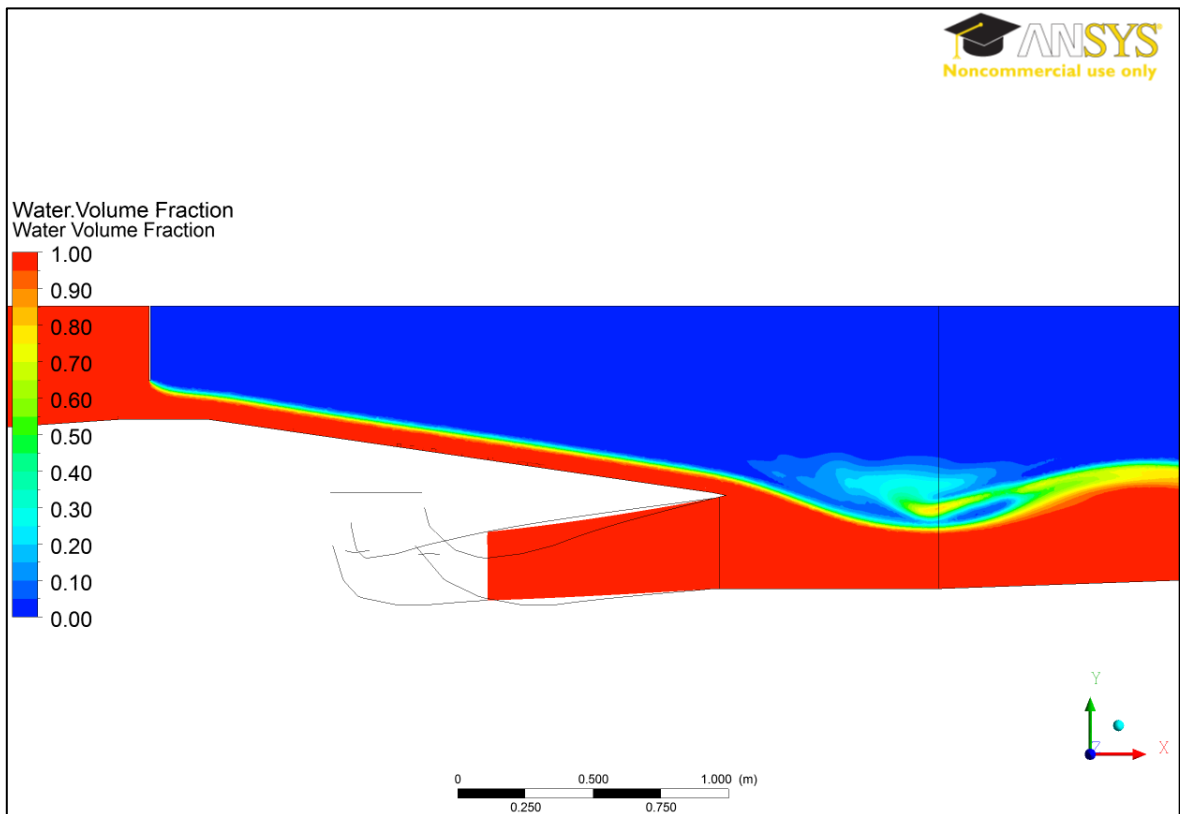


Figure 44. Water volume fraction (zoomed view) with 250 lit/s flow rate at the inlet.

Figure 45 shows the pressure contour at the inlet tank for this case.
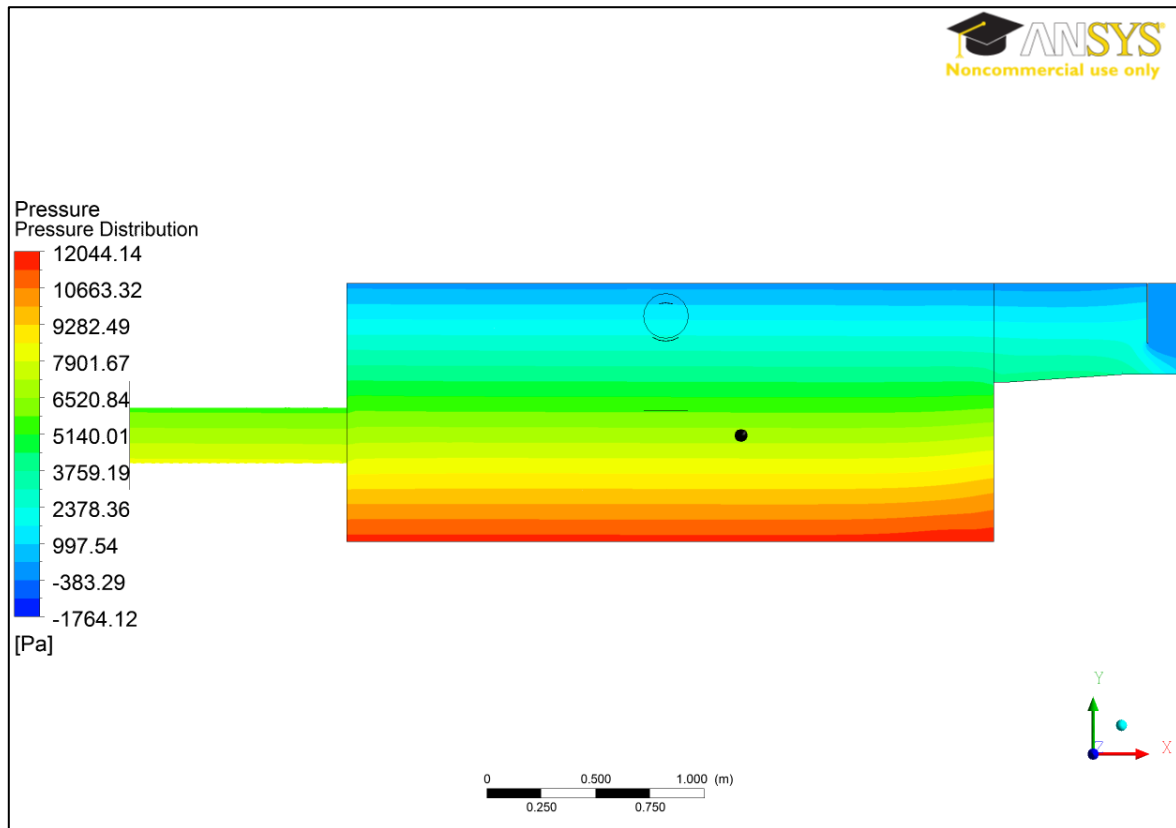


Figure 45. Pressure distribution in the inlet tank with ejector gate opened and 250 lit/s flow rate.

Here we have that the pressure at the dark point is 6857.05 Pascals. This value follows the decreasing trend seen in the previous cases and presents consistency with the reasoning behind this difference between results.

## 4. COMPARISON OF RESULTS

In order to validate the numerical results obtained, a comparison against the experimental results is performed. An important parameter for the characterization of the performance of the ejector ramp is the location in the $x$ and $y$ coordinates of the lowest point where the water from the draft tube mixes with the water from the ejector ramp. This point was visually measured in the experiments as it was previously shown in figure 5. As for the measure of this point in the numerical analysis, a polyline was created along the free surface and then computed into a XY plane-chart where these coordinates are easily obtained. Figure 46 shows the comparison of the numerical and experimental position of the lowest point in the mixing zone.
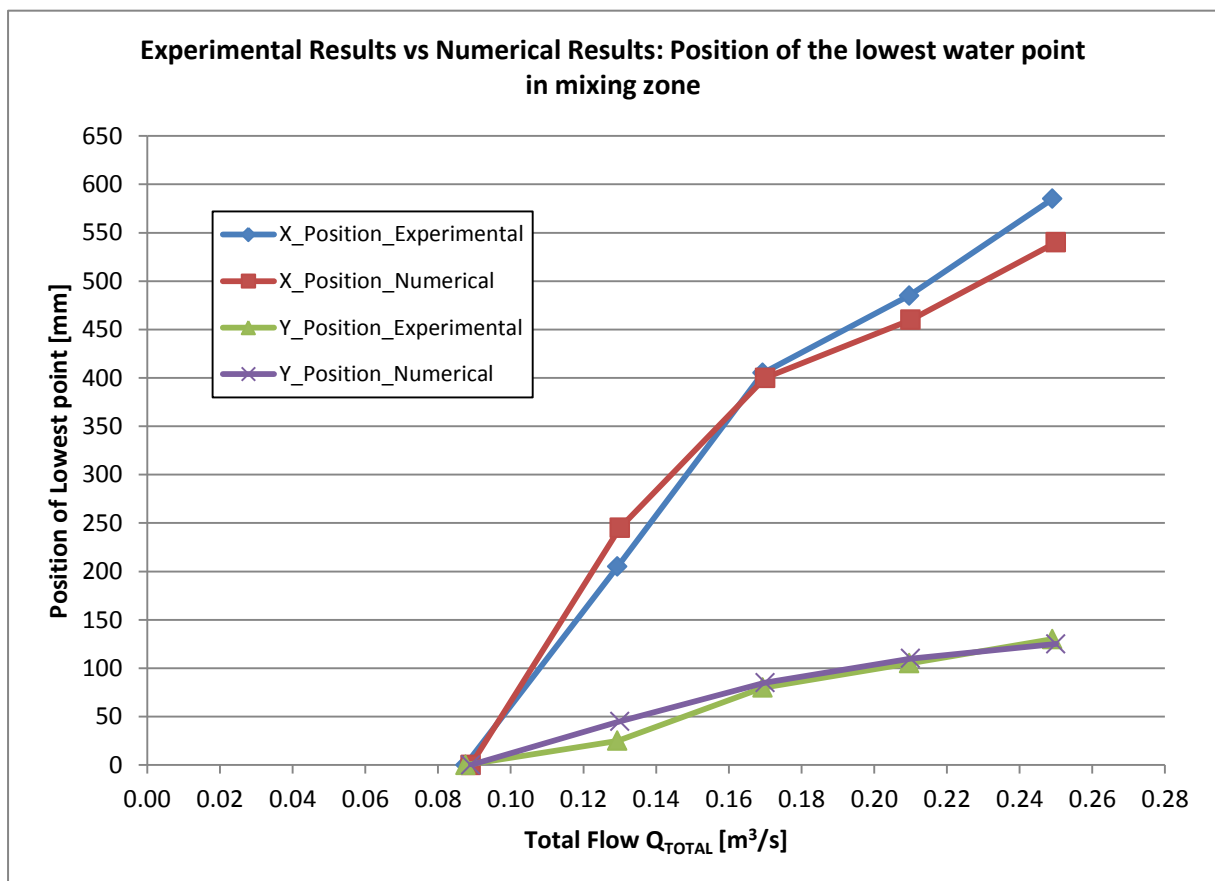


Figure 46. Position of the lowest water point in the mixing zone.

As it is possible to see in figure 46, the numerical results are in good agreement with the experimental results and therefore validate the effectiveness of numerical simulations.

The $y$ position in this figure represents the actual gain in head as a result of the ejector ramp effect. In this case we have that at the maximum flow rate analyzed we have an increment in head of around 18.5%.

A second comparison will be made in terms of $\Delta P_1$ and the flow rate in the turbine pipe. Figure 47 shows the results of the comparison for the four cases numerically tested.
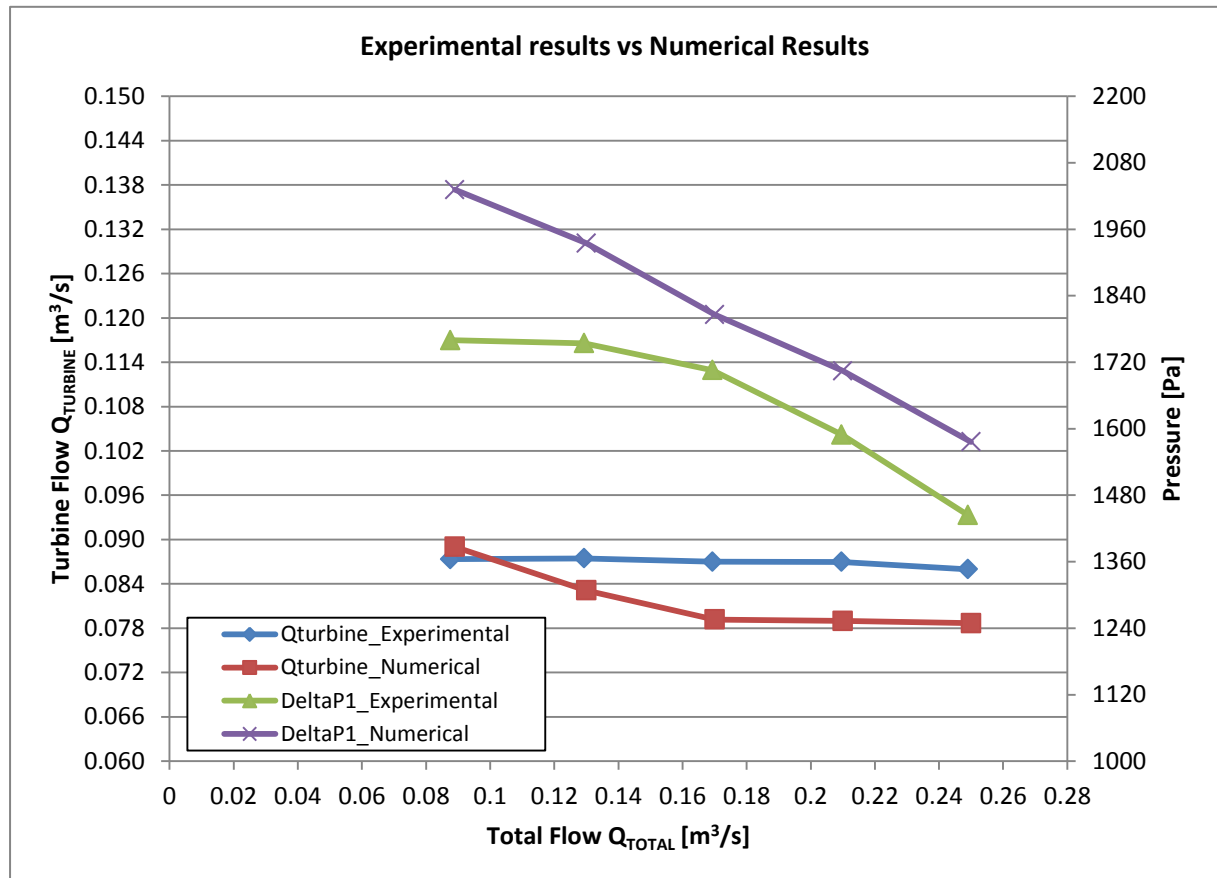


Figure 47. Comparison between experimental and numerical results.

In this figure we can see that the numerical results have the same trend than the experimental ones. However, there is a difference between results. In the numerical case, we have lower turbine flow rate than in the experimental case, being 9.2% the maximum difference, which occurs at 0.21 m$^3$/s. In the other hand, $\Delta P_1$ is higher in the numerical results. In this case, the maximum difference is the 15.5% and occurs at 0.089 m$^3$/s (ejector gate closed)

The reason behind this difference needs to be identified. At first, the relationship just found of higher pressure at the exit of the draft tube and lower turbine flow rate in the numerical case is

considered. These results actually make sense since higher pressure at the exit of the draft tube will create more resistance for the water to flow out of the draft tube and will reduce the amount of water in the turbine pipe. Therefore we will have less turbine flow rate. Based upon this relationship we can infer that the numerical results are valid since they are in accordance with the physics behind the model. Still, there is a difference in terms of results that needs to be considered. For this reason, it is necessary to analyze the boundary conditions, especially the ones in the inlet tank.

The inlet boundary condition was imposed to be the mass flow rate entering to the tank, and the free slip wall at top of the tank is intended to simulate the water free surface in this tank. However, from the analysis of the numerical results we found that the static pressure in inlet tank is slightly higher than the one theoretically expected. In order to analyze this effect, the pressure in the inlet tank at different total flow rates is graphically shown in figure 48.
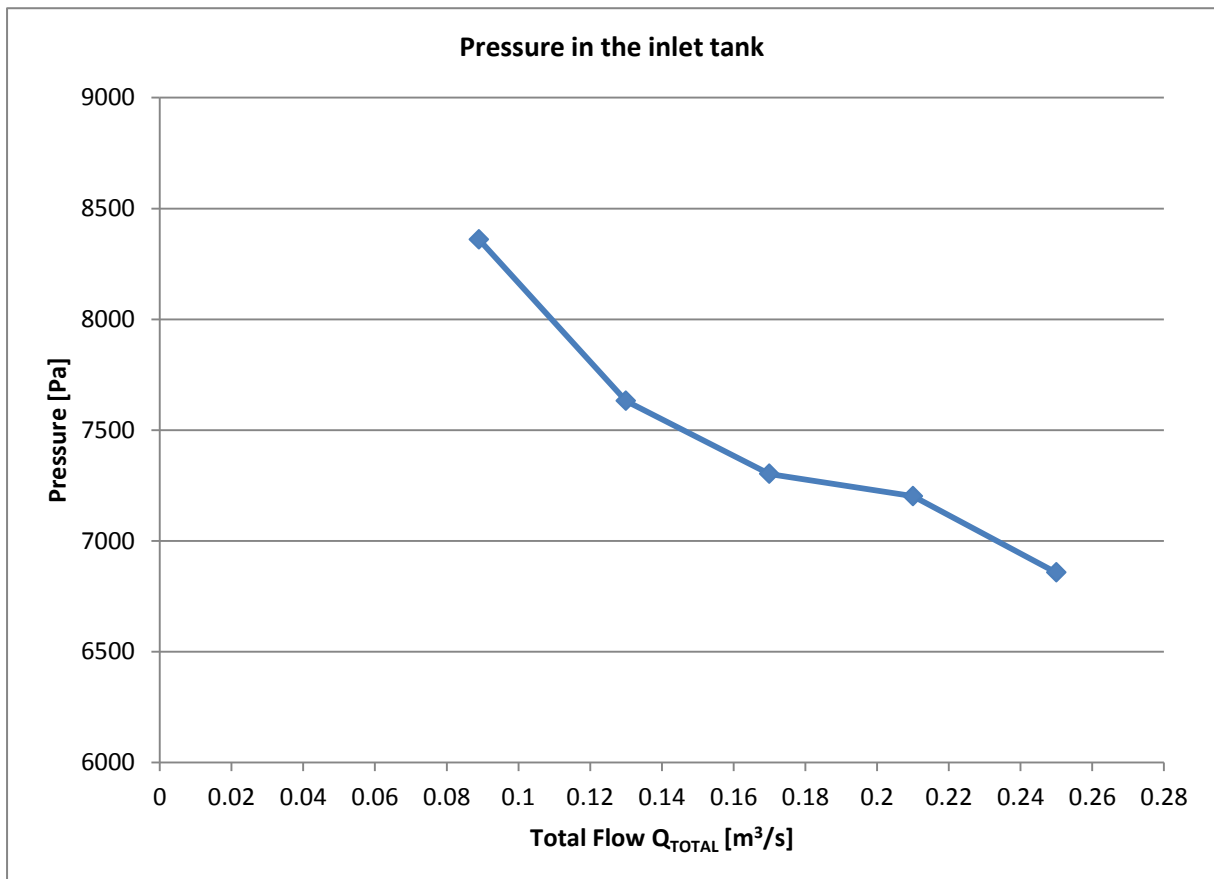


Figure 48. Pressure in the inlet tank.

In this figure we can see that as the total flow rate increases the static pressure in the virtual dark point in the inlet tank decreases. Since this static pressure is always measured at the same point, we

would theoretically expect values slightly oscillating around 7000 Pascals. A reason for this difference between results is the definition of the free slip boundary condition at the top of the inlet tank. In the experimental case, even when great effort is used, it is difficult to keep the upstream water level exactly constant at 700 millimeters. In addition, the flow rate at the inlet is also near impossible to keep it exactly at the desired value and without fluctuations. Therefore, in the numerical case we have that the inlet boundary condition is generating an equivalent to a slightly higher upstream water level. In order to validate this assumption, the equivalent head in the inlet tank for the numerical analysis is calculated based on the pressure obtained in the dark point. This calculation is carried out using the following equation

$$H = \frac{P}{\rho \cdot g}$$

Where $P$ is the pressure in the dark point, $\rho$ is the density of the water, and $g$ is the gravitational acceleration. Figure 49 shows the results obtained for the estimated head in the numerical analysis.
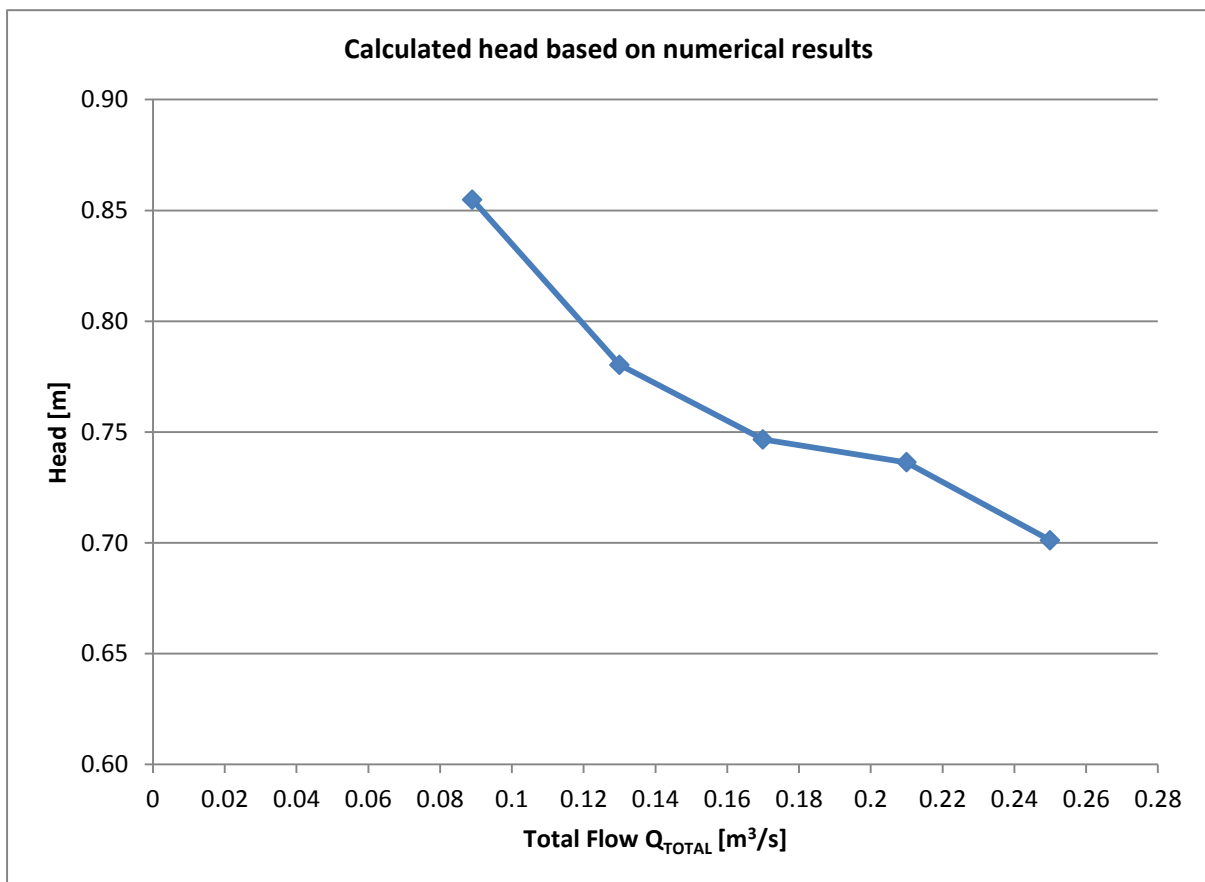


Figure 49. Calculated head in the inlet tank based on numerical results.

In this figure we can see that the upstream water level (head) is higher in the numerical cases than in the experiments. As expected it follows the same pattern of the pressure in the inlet tank and the equivalent head decreases as the total flow rate increases. Since the geometry is restricted in size and there is no room for the water to increase this level, it will result in an increment in pressure, which is seen in each numerical case analyzed. As the ejector gate is opened we see that pressure is released from the tank as more water is flowing down the ramp. For this reason, the way in what the free-slip wall boundary condition is imposed is generating overpressure in the inlet tank and affecting the turbine flow rate, therefore changing the conditions in the mixing flow zone and thus the pressure at the exit of the draft tube.

The difference in pressure and upstream water level becomes smaller in the case of 0.25 m$^3$/s, where we have almost the expected values. However, we still have difference between results in terms of turbine flow rate and $\Delta P_1$ and therefore another aspects will have to be taken into consideration.

Another factor that has to be included is the effect of friction in the walls. In the real case, we have different materials used to build the water district and hence different friction coefficients. In the case of the ejector gate and the region near the ramp we have changes in section as well as more complex geometry in real case than in the numerical one which represent a simplified version. Since in this case the geometry is constant and uniform and the walls are treated as smooth, water will find an easier way to flow down the ramp than in the real situation. This condition will generate differences and therefore explains the discrepancies between results.

The difference found for the numerical analysis will create changes in the hydraulic power output is this value was to be computed. In order to achieve more accurate results, the imposition of the boundary conditions will have to be modified to include conditions that replicate in a better way to the real conditions of the model tested

Despite the difference in the results for some of the characteristics measured, the computational results are considered as valid since they are in good agreement with the physics behind the problem. Also the differences found are within an acceptable range for engineering applications and therefore it satisfies the expectations of the tool as a way of testing real hydropower plants conditions.

As a final step, it is necessary to compute the benefits of the implementation of the ejector ramp under several working conditions.

For this reason, Figure 49 shows a hill chart of the percentage of increment in hydraulic power as a function of the tail water level characteristics of the river where the power plant is installed at. This figure is only based on the experimental results obtained in this study.
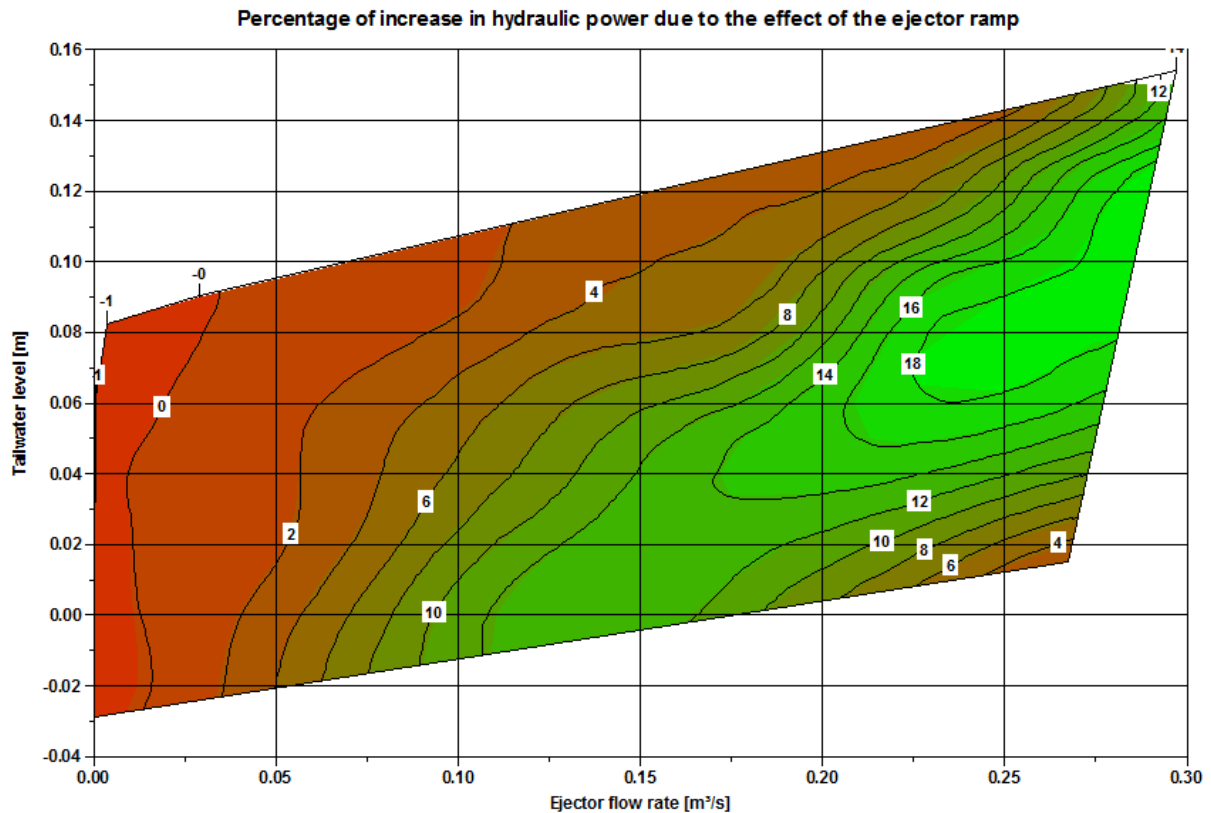


Figure 50. Percentage of increment in hydraulic power due the implementation of the ejector ramp.

In this figure, we can see that the top and bottom lines have a slope which corresponds to the slope seen in the tailwater level when this increases at higher total flow rate. The lowest value in the Y axis is -30 millimeters and the highest value in this same axis is 80 millimeters. These values correspond to the top and bottom values for the initial tailwater levels tested.

The green zone in figure 48 represents the maximum positive effect of the ejector ramp, where we can get up to 18% increase in the total hydraulic power. As it can be seen in this figure, this maximum positive effect happens with higher ejector flow rate. This result is expected since higher flow rates in the ramp means higher flow velocities when moving down the ramp. These velocities contribute positively to decrease the pressure at the exit of the draft tube and therefore increase the flow rate through the turbine and hence the power generated. It has to be considered that the

tailwater level also plays a role in this chart. As this characteristic varies from river to river, it is required that the tailwater slope passes by the region of higher percentage of increment in power. Matching this slope with the adequate ejector flow rate will produce optimum results for the ejector ramp in the hydraulic power plant. Although these results are based on a scaled-water district, using the powerful fluid dynamics tool known as similarity laws these results can be scaled to real size hydropower plants.

# 5. CONCLUSIONS.

- In the present study the effect of the ejector ramp as an effective head increaser for low-head hydropower plants using Kaplan turbines was successfully studied under different conditions such as inlet total flow rate and different tailwater levels. The evaluation in this study was carried out using experimental and numerical approaches and was intended to compare results for future evaluations.

- In the experimental analysis it was found that the initial tail water level of the power plants has a significant influence in the total hydraulic power output. Lower initial tailwater levels will result in higher average power output. However, it is noted that this condition cannot be deliberately put into practice without the adequate analysis of this effect in the performance and design condition of the Kaplan turbine used at the specific location.

- It was found that the water flow rate in the ejector ramp has an important influence in the overall effect of the ejector ramp. Higher water flow in the ejector ramp will increase its positive effect on the overall performance of the power plant. It was also found that the initial tailwater level and the ejector mass flow rate could be related to each other when estimating the increase in power output due to the effect of the ejector ramp. These results were conveniently plotted into a hill chart for a wide range of conditions and the results can be scaled to real power plants using similarity laws.

- The results of this study can be used to determine when the ejector ramp can be implemented in existing low-head hydropower plants. Knowing the characteristic behavior of the tailwater level and the excess of water obtained in the river during rainy seasons, it will be possible to compute the increment in power output based on the results here obtained and therefore perform the economic analysis of the construction project.

- The numerical analysis performed on the ejector ramp showed slight differences in relation with the experimental case. These differences are found to be in an acceptable range and therefore the numerical results proved to be realistic. In addition, the causes of this differences where identified and explained in the discussion of the numerical results. Modifications on the boundary conditions, especially the top-wall of the inlet tank will allow

obtaining more accurate results. Performing the analysis in transient mode will incur in higher computational time but will provide a better approximation to the real case.

- The procedure explained and followed for the numerical analysis is considered valid and therefore can be implemented if any modification is to be made into the original geometry of the ejector ramp analyzed in this study.

- In summary, based on the result of this study it was proven that the ejector ramp has an overall positive effect as an effective head increaser in low-head hydropower plants using Kaplan turbines.

- As a personal conclusion, this project allowed to expand my knowledge in the field of hydropower, hydraulic machines, and numerical analysis by means of Computational Fluid Dynamics (CFD). This opportunity provided me with a better understanding of how research is conducted and allowed me to interact with highly experience professors and students in this field, as well as to perform experimental analysis that has a direct applicability to the industry. Besides all the academic knowledge I acquired through this experience, it also gave me the opportunity to get involved with the Austrian culture which I found amazing and very interesting. To summarize, this was a remarkable experience that made me grow academically, professionally, and personally.

# 6. REFERENCES

[1] Mosonyi, E., ***Low-head hydropower plants. Volume One.*** Third enlarged and completely revised edition. Akademiai Kiado, Budapest. 1987

[2] Kothandaraman, C.P., ***Fluid Mechanics and Machinery.*** Second Edition. New Age International Publishers. 2007

[3] Ansys CFX Theory Guide. Release 15.0. November 2013.